IEEE Access
Multidisciplinary | Rapid Review | Open Access Journal

Received March 24, 2019, accepted April 6, 2019, date of publication April 11, 2019, date of current version April 25, 2019.

Digital Object Identifier 10.1109/ACCESS.2019.2910325

Configuration Optimization for Manipulator Kinematic Calibration Based on Comprehensive Quality Index

GANG CHEN, (Member, IEEE), LEI WANG, BONAN YUAN, AND DAN LIU
School of Automation, Beijing University of Posts and Telecommunications, Beijing 100876, China

Corresponding author: Gang Chen (buptcg@163.com)

This work was supported in part by the National Natural Science Foundation of China under Grant 61403038 and Grant 61573066, and in part by the Research Fund of the Manned Space Engineering under Grant 18051030101.

ABSTRACT Kinematic calibration performance is heavily dependent on two factors–the ability of calibration configurations mapping kinematic parameter errors, and the un-modeled errors including joint clearance, thermal expansion, and measurement noise. Therefore, this paper deals with the calibration configuration optimization to reduce the impact of the two factors on calibration performance. We pay particular attention to establish an index for evaluating calibration configuration's quality. Different from other works, the proposed comprehensive quality index can simultaneously reflect configurations' observability and globality. Furthermore, the numerical methods are used to analyze the relationships between the comprehensive quality index and configuration number, and the relationships between calibration performance and configuration number. Based on the above relationships, we provide a feasible solution for determining the calibration configuration number of a specific manipulator. Based on the above work, configuration optimization model is established and solved by particle swarm optimization. The simulation of an eight degree-of-freedom manipulator illustrates the advantages of the proposed method. In 100 calibration simulations, optimized configurations perform better than random configurations, with the position accuracy increased by 43.86% and the attitude accuracy increased by 14.29%.

INDEX TERMS Calibration configuration, comprehensive quality index, kinematic calibration, particle swarm optimization.

I. INTRODUCTION

In the study of manipulator, scholars have carried out many studies to reduce kinematic parameter errors, and kinematic calibration methods with increasingly maturity have become a universal solution [1]–[3]. Based on existing studies, kinematic calibration can improve the positioning accuracy of a manipulator about an order of magnitude [4]–[6]. However, the position/attitude accuracy after calibration is sometimes still difficult to meet the requirements of typical operation tasks such as precision machining and microsurgery. This phenomenon is caused by two factors. One of the factors is the existence of un-modeled errors [7], including joint clearance [8], thermal expansion [9], and measurement noise [10]. Although these un-modeled errors occupy a small proportion in the positioning error of manipulator, they will significantly affect calibration performance [11]. In fact, the un-modeled errors are difficult to eliminate. Considering the effects of the un-modeled errors are different when using different configurations in calibration, we can reduce the impact of the un-modeled errors by choosing appropriate calibration configurations. Another factor is the difference in the ability of different calibration configurations to map kinematic parameter errors. Good configurations can evenly map all kinematic parameter errors to end position/attitude errors, which are beneficial to improve calibration performance. For the above two reasons, it is necessary to find an optimal configuration set to reduce negative effects of the un-modeled errors and to map kinematic parameter errors better.

In order to optimize calibration configurations, scholars established many indexes to evaluate the quality of

The associate editor coordinating the review of this manuscript and approving it for publication was Seyedali Mirjalili.

configurations, and developed algorithms that are suitable for configuration optimization.

The end position/attitude errors of a manipulator will form an ellipsoid when parameter errors are constant, and singular values of error Jacobian matrix determine the ellipsoid's boundary. Therefore, the singular values can measure the configurations' observability on kinematic parameters [12]. Based on the singular value decomposition (SVD) of error Jacobian matrix, most of the indexes for evaluating calibration configurations are established. There are six most common indexes. One of the indexes is observability index (expressed as O_1) [13]. O_1 is calculated by geometric mean of singular values. It reflects the overall observability of configurations. The second index is condition number (expressed as O_2) [14]; it reflects the average observability of configurations. The third index is minimum singular value (expressed as O_3) [15]; it reflects the worst observability of configurations. The forth index is noise amplification index (expressed as O_4) [16]; it combines the performance of O_2 and O_3. The fifth index is based on A-optimal design (expressed as O_5) [17]; it also reflects the overall observability of configurations. The newest index is improved Φ_p-optimality index (is expressed as O_6) [11], and both O_1, O_3, and O_5, can be regarded as special cases of O_6.

From the above studies, we could find that there are many indexes to evaluate calibration configurations' quality. However, each existing index focuses on partial aspects of configurations' observability. Actually, calibration requires a set of configurations that has the best comprehensive ability to observe kinematic parameter errors. Therefore, we need to integrate existing indexes to select configurations with the best observability. In addition to observability, we also need to consider another performance that is called configurations' globality. The manipulator's residual end position/attitude errors of different configurations can be calculated by calibrated parameters. These residual end position/attitude errors are calibration residuals. The calibration residuals are smallest for the calibration configurations, but are bigger for other configurations. It is because the essence of kinematic calibration is to approximate the actual value of kinematic parameters using calibration configurations as sample points. The selection of the sample points determines the accuracy of the calibrated parameters. The above characteristic of calibration configurations is the configurations' globality. Therefore, in order to improve calibration performance, it is also necessary to improve the globality of calibration configurations. By establishing an index that can simultaneously evaluate observability and the globality of calibration configurations, we can select out a set of configurations that have the best calibration performance.

After establishing index to evaluate configurations' quality, the next step is to design configuration optimization algorithm. Scholars have applied many algorithms to optimize configurations, including DETMAX [18]–[20], simulated annealing (SA) [21], genetic algorithm (GA) [22]–[23], particle swarm optimization (PSO) [11], etc. DETMAX [24] is one of the most widely used algorithms for calibration configuration optimization. However, because DETMAX needs to perform operations such as ''add-compare-exchange-delete'' one by one for alternative configurations, the calculation is complicated and the efficiency is low, especially when the number of alternative configurations is large. To improve efficiency, one of the methods uses configuration perturbation to optimize configurations, and uses a small amount of DETMAX's operations to avoid local optimal solution [25]. However, this method is complicated to implement. Another method uses GA with gradient search; it uses parallel computing to accelerate optimization process, and uses repetitive configurations to reduce the dimension of calculation [23]. However, repetitive configurations are easy to make error Jacobian matrix be singular. As a kind of swarm intelligence algorithm, PSO has the characteristics of fast convergence, simple modeling, and easy implementation. Compared with other optimization algorithms, PSO requires fewer parameters and can achieve better results in a faster and low-cost way [11]. Therefore, in order to optimize configurations efficiently, this paper chooses the PSO to solve optimization model of calibration configuration.

In summary, we need to find an optimal calibration configuration set to reduce effects of the un-modeled errors and yield the best observability of kinematic parameter errors. In order to achieve the goal, it is necessary to establish an index to evaluate the quality of calibration configurations. The existing indexes only evaluate configurations' observability from some single perspective, and they never discuss the globality of configurations. For this reason, this paper explores a method to evaluate configurations' globality, and establish a comprehensive quality index. Based on the index, this paper considers constraints of configuration number and joint angle limits, and uses PSO to solve optimization model of calibration configuration. The contributions of this paper mainly include the following points:

- We establish configurations' dispersion index and evenness index by considering distribution of manipulator's end points in workspace. These indexes can be used to obtain configurations with a better globality.
- By combining the existing observability indexes with globality indexes, we propose a comprehensive quality index, which can simultaneously reflect the calibration configurations' observability and globality.
- Numerical methods are used to analyze the relationships between comprehensive quality index and configuration number, and the relationships between calibration accuracy and configuration number. Based on the relationships, we provide a feasible solution for determining calibration configuration number for a specific manipulator.

The rest of this paper is organized as follows: Section II analyzes factors that affect calibration performance. Section III establishes the comprehensive quality index to evaluate configurations. Section IV designs a method to optimize configurations based on PSO. Section V shows

simulation results of proposed methods. Section VI summarizes research results and provides future research directions.

II. FACTORS AFFECTING CALIBRATION PERFORMANCE

Kinematic calibration performance is heavily dependent on the ability of calibration configurations mapping kinematic parameter errors, and the effects of the un-modeled errors. Before optimize configurations, we first need to analyze how these factors influence the calibration performance.

A. EVALUATE CALIBRATION PERFORMANCE

The kinematic model of manipulator is the basis for kinematic calibration. We can use kinematic model to obtain end position/attitude in any configuration of a manipulator. (In order to make the analysis process more concise, this section replaces the complete expressions of the kinematic model and kinematic error model of the manipulator with the simplified expressions. The modeling process and complete expressions are shown in Appendix.)

The end position/attitude can be expressed as a function of kinematic parameters and joint angles, as shown in (1).

$$\boldsymbol{P}^{\mathrm{N}} = f(\boldsymbol{\Omega}^{\mathrm{N}}, \boldsymbol{\theta}) \tag{1}$$

where $\boldsymbol{P}^{\mathrm{N}} \in \Re^6$ is the nominal value of end position/attitude; $\boldsymbol{\Omega}^{\mathrm{N}} \in \Re^{np}$ is the nominal value of kinematic parameters; n is degrees-of-freedom (DOF); p is the number of parameters used to describe the relationship between two adjacent link coordinate systems; $\boldsymbol{\theta} = [\theta_1, \theta_2, \cdots, \theta_n] \in \Re^n$ is a set of joint angles.

However, actual value of kinematic parameters is often different from nominal value, because the existence of manufacturing errors, assembly errors, environmental changes and other factors. This deviation leads to a change in end position/attitude. We can express actual value of end position/attitude $\boldsymbol{P}^{\mathrm{A}}$ as

$$\boldsymbol{P}^{\mathrm{A}} = f(\boldsymbol{\Omega}^{\mathrm{A}}, \boldsymbol{\theta}) \tag{2}$$

where $\boldsymbol{\Omega}^{\mathrm{A}} \in \Re^{np}$ is actual value of kinematic parameters, which cannot be measured.

The kinematic error model can be established by (1) and (2). The model reflects relationship between end position/attitude errors and kinematic parameter errors, as shown in (3).

$$\lim_{\Delta\boldsymbol{\Omega}\to 0} \frac{\Delta \boldsymbol{P}}{\Delta \boldsymbol{\Omega}} = \frac{\mathrm{d}\boldsymbol{P}^{\mathrm{N}}}{\mathrm{d}\boldsymbol{\Omega}^{\mathrm{N}}} \tag{3}$$

where $\Delta \boldsymbol{P} = \boldsymbol{P}^{\mathrm{A}} - \boldsymbol{P}^{\mathrm{N}}$ is deviation between actual value and nominal value of end position/attitude; $\Delta\boldsymbol{\Omega} = \boldsymbol{\Omega}^{\mathrm{A}} - \boldsymbol{\Omega}^{\mathrm{N}}$ is deviation between actual value and nominal value of kinematic parameters.

The right side of (3) is error Jacobian matrix, and it can be expressed as $\boldsymbol{J}$ ($\boldsymbol{J} \in \Re^{6\times np}$), as shown in (4).

$$\boldsymbol{J} = \frac{\mathrm{d}\boldsymbol{P}^{\mathrm{N}}}{\mathrm{d}\boldsymbol{\Omega}^{\mathrm{N}}} \tag{4}$$

Then, kinematic calibration can be described as follows. We continuously calculate kinematic parameter errors through multiple iterations, until the deviation between calculated value and measured value of end position/attitude is less than an expected threshold, as shown in (5).

$$f(\Delta\boldsymbol{\Omega}) = \sum_{i=1}^{m} \|\Delta \boldsymbol{P}_i - \boldsymbol{J}_i \cdot \Delta\boldsymbol{\Omega}\|^2 \le \boldsymbol{\varepsilon} \tag{5}$$

where $\Delta \boldsymbol{P}_i$ is end position/attitude errors of the i-th configuration obtained by measurement; $\boldsymbol{J}_i$ is error Jacobian matrix of the i-th configuration; m is configuration number, which usually depends on the calibration requirements; $\boldsymbol{\varepsilon}$ is an expected threshold.

In order to implement the above process, we can use least squares method to solve kinematic parameter errors. Let $\bar{\boldsymbol{J}} = \left[\boldsymbol{J}_1^{\mathrm{T}}, \boldsymbol{J}_2^{\mathrm{T}}, \cdots, \boldsymbol{J}_m^{\mathrm{T}}\right]^{\mathrm{T}}$ ($\bar{\boldsymbol{J}} \in \Re^{6m\times np}$), $\Delta\bar{\boldsymbol{P}} = \left[\Delta\boldsymbol{P}_1^{\mathrm{T}}, \Delta\boldsymbol{P}_2^{\mathrm{T}}, \cdots, \Delta\boldsymbol{P}_m^{\mathrm{T}}\right]^{\mathrm{T}}$ ($\Delta\bar{\boldsymbol{P}} \in \Re^{6m}$), then kinematic calibration equation can be expressed as

$$\Delta\boldsymbol{\Omega}' = \left(\bar{\boldsymbol{J}}^{\mathrm{T}}\bar{\boldsymbol{J}}\right)^{-1} \cdot \bar{\boldsymbol{J}}^{\mathrm{T}} \cdot \Delta\bar{\boldsymbol{P}} \tag{6}$$

where $\Delta\boldsymbol{\Omega}'$ is calibrated kinematic parameter errors.

The calibrated kinematic parameters $\boldsymbol{\Omega}^{\mathrm{C}}$ can be expressed as

$$\boldsymbol{\Omega}^{\mathrm{C}} = \boldsymbol{\Omega}^{\mathrm{N}} + \Delta\boldsymbol{\Omega}' = \boldsymbol{\Omega}^{\mathrm{N}} + \left(\bar{\boldsymbol{J}}^{\mathrm{T}}\bar{\boldsymbol{J}}\right)^{-1} \cdot \bar{\boldsymbol{J}}^{\mathrm{T}} \cdot \Delta\bar{\boldsymbol{P}} \tag{7}$$

The residual deviation between actual value and calibrated value of kinematic parameters $\delta\boldsymbol{\Omega}$ is

$$\delta\boldsymbol{\Omega} = \boldsymbol{\Omega}^{\mathrm{A}} - \boldsymbol{\Omega}^{\mathrm{C}} = \Delta\boldsymbol{\Omega} - \Delta\boldsymbol{\Omega}' \tag{8}$$

This deviation is a direct index to evaluate calibration performance. However, we cannot obtain exact value of the residual deviation, because we cannot measure actual kinematic parameters. The end position/attitude corrected by calibrated parameters also has a deviation from actual value. Therefore, we can measure calibration performance by the end position/attitude errors after calibration.

For a configuration $\boldsymbol{\theta}$ ($\boldsymbol{\theta} = [\theta_1, \theta_2, \cdots, \theta_n] \in \Re^n$) of manipulator, the end position/attitude corrected by calibrated parameters is

$$\boldsymbol{P}^{\mathrm{C}} = f(\boldsymbol{\Omega}^{\mathrm{C}}, \boldsymbol{\theta}) \tag{9}$$

where $\boldsymbol{P}^{\mathrm{C}} \in \Re^6$ is corrected nominal value of end position/attitude.

We call deviation between actual value and corrected nominal value of end position/attitude as the calibration residuals $\delta\boldsymbol{P}$, which can be expressed as (10).

$$\delta\boldsymbol{P} = \boldsymbol{P}^{\mathrm{A}} - \boldsymbol{P}^{\mathrm{C}} = \boldsymbol{P}^{\mathrm{A}} - f(\boldsymbol{\Omega}^{\mathrm{C}}, \boldsymbol{\theta}) \tag{10}$$

Then, we can evaluate calibration performance using (10).

B. FACTORS AFFECTING CALIBRATION PERFORMANCE

Equation (7) shows that calibrated parameters are calculated by end position/attitude errors and error Jacobian matrix. (1), (2) and (4) show that end position/attitude errors and error Jacobian matrix are both functions of calibration configurations. Therefore, from (10) we can know that calibration residuals are a function of calibration configurations.

$$\delta \boldsymbol{P} = f(\bar{\boldsymbol{\theta}}) \tag{11}$$

where $\bar{\boldsymbol{\theta}} = \{\boldsymbol{\theta}_1, \boldsymbol{\theta}_2, \cdots, \boldsymbol{\theta}_m\}$ is a collection of calibration configurations.

A set of configurations contains two pieces of information. One is the number of configurations, and the other is the joint angles. They all affect calibration residuals.

First, we discuss the impact of configuration number on calibration. The end position/attitude is a six-dimensional vector, so we have $6m$ kinematic calibration's equations when the configuration number is m. If kinematic model describes relationship between two manipulator's link coordinate systems with p parameters, an n-DOF manipulator contains np kinematic parameters (i.e., np unknown variables). Only when $6m \geq np$ (i.e. the number of equations equals or is greater than the number of unknowns) can we obtain the unique solution or least square solution of the kinematic parameter error. Therefore, it is necessary to determining appropriate number of configurations for kinematic calibration process.

We also need to discuss the impact of joint angles on calibration. The calibration residuals are smallest for calibration configurations, but are bigger for other configurations. It is because kinematic calibration's essence is to approximate actual value of kinematic parameters using calibration configurations. The selection of calibration configurations determines accuracy of calibrated parameters. We use globality to define the above characteristics of calibration configurations. If calibration configurations concentrate in an area, configurations' globality will be poor, and calibrated parameters will only improve position/attitude accuracy of manipulator in local workspace.

Furthermore, error Jacobian matrixes corresponding to different configurations are different. The mathematical characteristics of error Jacobian matrix will affect solution of calibration equations. We use r represents rank of error Jacobian matrix. According to whether error Jacobian matrix is full rank or not, the following four situations occur:

- The error Jacobian matrix is full column rank (i.e. $r = np$). In this case, all kinematic parameters are linearly independent, i.e. there are no redundant parameters. When configurations number is sufficient, all kinematic parameters can be solved.
- The error Jacobian matrix is full row rank (i.e. $r = 6m$). In this case, all configurations are linearly independent; calibration equations have solutions (possibly multiple set of solutions).
- The error Jacobian matrix is a full rank square matrix (i.e. $r = 6m = np$). In this case, both kinematic parameters and configurations are linearly independent, and calibration equations only have one set of solutions.
- Both column rank and row rank of error Jacobian matrix are rank deficient (i.e. $r < 6m$, $r < np$). In this case, some kinematic parameters are linearly dependent, some configurations are linearly dependent, and calibration equations do not have solution or have multiple set of solutions.

Based on the above analysis, we summarize impacts of calibration configurations on calibration process as follows:

- The configuration number will affect solution of calibration equations. Only the configuration number satisfying the condition $6m \geq np$ can solve valid parameters.
- The selection of calibration configurations determines similarity of calibrated parameters and actual parameters.
- The joint angles of configurations will affect error Jacobian matrix. The solvability of calibration equations corresponding to different error Jacobian matrices is different.

III. COMPREHENSIVE QUALITY INDEX OF CALIBRATION CONFIGURATIONS

Based on the above analysis, we will evaluate the calibration configurations from both the observability and globality.

A. CONFIGURATIONS' OBSERVABILITY INDEXES

Different configurations correspond to different error Jacobian matrix, and have different observability. Therefore, we can establish configurations' observability index based on the mathematical characteristics of error Jacobian matrix.

Singular values reflect mathematical characteristics of error Jacobian matrix, so they indirectly reflect the quality of configurations. We can obtain singular values by SVD. For example, the SVD of an error Jacobian matrix $\boldsymbol{J}$ in $q \times s$ dimension is expressed as

$$[\boldsymbol{U}, \boldsymbol{\Sigma}, \boldsymbol{V}^{\mathrm{T}}] = \mathrm{SVD}(\boldsymbol{J}) \tag{12}$$

where $\boldsymbol{U}\boldsymbol{\Sigma}\boldsymbol{V}^{\mathrm{T}} = \boldsymbol{J}$; the matrixes $\boldsymbol{U} \in \Re^{q\times q}$ and $\boldsymbol{V} \in \Re^{s\times s}$ are orthogonal matrix; the matrix $\boldsymbol{\Sigma} \in \Re^{q\times s}$ is singular value matrix of $\boldsymbol{J}$, and it can be expressed as

$$\boldsymbol{\Sigma} = \begin{bmatrix} \lambda_1 & 0 & \cdots & 0 \\ 0 & \lambda_2 & \cdots & 0 \\ \vdots & \vdots & \ddots & \vdots \\ 0 & 0 & \cdots & \lambda_s \\ 0 & 0 & \cdots & 0 \\ \vdots & \vdots & \ddots & \vdots \\ 0 & 0 & \cdots & 0 \end{bmatrix} \tag{13}$$

where $\lambda_1, \lambda_2, \cdots, \lambda_s$ are singular values of $\boldsymbol{J}$, and satisfy the relationship of $\lambda_1 \geq \lambda_2 \geq \cdots \geq \lambda_s \geq 0$.

Then the general formula of the existing indexes can be expressed as

$$O = f(\boldsymbol{\Sigma}) \tag{14}$$

where O is index that evaluate configuration's observability.

Based on singular values of error Jacobian matrix, we obtain the following indexes:

- The observability index O_1: This index is calculated by geometric mean of singular values. It performs as volume of the space created by discrete data, and can measure overall observability of configurations. The larger the O_1, the better the overall observability on kinematic parameter errors.

$$O_1 = \frac{(\lambda_1 \lambda_2 \cdots \lambda_s)^{1/s}}{\sqrt{s}} \tag{15}$$

- The condition number O_2: This index is calculated from ratio of the minimum singular value to the maximum singular value. It reflects uniformity of discrete data in all directions, and can measure average observability of configurations. The larger the O_2, the better the average observability on kinematic parameter errors; When $O_2 = 1$, configurations have the best average observability.

$$O_2 = \frac{\lambda_s}{\lambda_1} \tag{16}$$

- The minimum singular value O_3: This index reflects the worst observability of all configurations. The larger the O_3, the better the observability on kinematic parameter errors.

$$O_3 = \lambda_s \tag{17}$$

Based on definitions of the above three observability indexes, when homogeneity [26] of selected configurations is good, O_1, O_2, O_3 are close to a fixed value.

The above observability indexes evaluate configurations' observability from different aspects, and we need to integrate existing indexes to select a set of configurations with the best comprehensive observability.

B. CONFIGURATIONS' GLOBALITY INDEXES

In addition to observability, we also need to consider configurations' globality. The globality can be evaluated by the spatial distribution of the configurations. On the one side, a set of configurations should be dispersive in space, because parameters calibrated by dispersive configurations are more applicable in the entire workspace. On the other side, a set of configurations should be even in space, because parameters calibrated by even configurations can improve position/attitude accuracy evenly in the entire workspace. For these reasons, we establish the following dispersion and evenness index.

1) CONFIGURATIONS' DISPERSION INDEX

The configuration's dispersion index can be calculated by dispersion of manipulator's end points. Variance can measure the dispersion of a finite points set.

Suppose $\boldsymbol{A} = \{\boldsymbol{x}_1, \boldsymbol{x}_2, \cdots, \boldsymbol{x}_{N_A}\}$ is a point set in d-dimensional space $\boldsymbol{S}^d$ (i.e. $\boldsymbol{x}_i \in \boldsymbol{S}^d$). $N_{\boldsymbol{A}}$ is points number. The center point $\boldsymbol{x}_{\mathrm{C}}$ of the points set $\boldsymbol{A}$ (i.e. arithmetic mean of coordinates of points) is

$$\boldsymbol{x}_{\mathrm{C}} = \frac{1}{N_{\boldsymbol{A}}} \sum_{i=1}^{N_A} \boldsymbol{x}_i \tag{18}$$

Then, variance of points set $\boldsymbol{A}$ is

$$D(\boldsymbol{A}) = \frac{1}{N_{\boldsymbol{A}}} \sum_{i=1}^{N_A} (\boldsymbol{x}_i - \boldsymbol{x}_{\mathrm{C}})^{\mathrm{T}} (\boldsymbol{x}_i - \boldsymbol{x}_{\mathrm{C}}) \tag{19}$$

$D(\boldsymbol{A})$ is the dispersion of points set $\boldsymbol{A}$. The bigger the $D(\boldsymbol{A})$, the better the dispersion of the point set.

The end point set corresponding to configuration set $\bar{\boldsymbol{\theta}} = \{\boldsymbol{\theta}_1, \boldsymbol{\theta}_2, \cdots, \boldsymbol{\theta}_m\}$ is $\{\boldsymbol{P}_{d_1}, \boldsymbol{P}_{d_2}, \cdots, \boldsymbol{P}_{d_m}\}$ $(\boldsymbol{P}_{d\_i} \in \Re^3)$. Then the dispersion of configurations $\bar{\boldsymbol{\theta}}$ can be calculated as

$$\begin{aligned} D(\bar{\boldsymbol{\theta}}) &= \frac{1}{m} \sum_{i=1}^{m} \left(\boldsymbol{P}_{d\_i} - \boldsymbol{P}_{d\_\mathrm{C}}\right)^{\mathrm{T}} \left(\boldsymbol{P}_{d\_i} - \boldsymbol{P}_{d\_\mathrm{C}}\right) \\ &= \frac{1}{m} \sum_{i=1}^{m} \left(\boldsymbol{P}_{d\_i}(\boldsymbol{\theta}_i) - \frac{1}{m} \sum_{i=1}^{m} \boldsymbol{P}_{d\_i}(\boldsymbol{\theta}_i)\right)^{\mathrm{T}} \\ &\quad \times \left(\boldsymbol{P}_{d\_i}(\boldsymbol{\theta}_i) - \frac{1}{m} \sum_{i=1}^{m} \boldsymbol{P}_{d\_i}(\boldsymbol{\theta}_i)\right) \end{aligned} \tag{20}$$

We can evaluate configurations' dispersion by (20). The bigger the $D(\bar{\boldsymbol{\theta}})$, the better the dispersion of configurations.

Fig. 1 shows different values of dispersion in two-dimensional space. Fig. 1(a) shows when end points corresponding to configurations are all focus on one point, the dispersion reaches the minimum value 0. Fig. 1(b) shows when end points are located at boundary of workspace, the dispersion reaches the maximum value r_S (i.e. radius of workspace). Fig. 1(c) shows when configuration number approaches infinity and end points fill entire workspace, the dispersion approaches a constant value $r_S/2$.

2) CONFIGURATIONS' EVENNESS INDEX

The configuration's evenness index can be calculated by evenness of the manipulator's end points. The following method can measure evenness of a finite point set [27].

The average distance d_{ave} between each point and center point $\boldsymbol{x}_{\mathrm{C}}$ in points set $\boldsymbol{A}$ is standard deviation of points' coordinates, shown as (21)

$$d_{\mathrm{ave}} = \sqrt{D(\boldsymbol{A})} \tag{21}$$

Take a random point $\boldsymbol{y}$ in space $\boldsymbol{S}^d$. We can calculate the minimum distance between $\boldsymbol{y}$ and all points in points set $\boldsymbol{A}$. The minimum distance can be expressed as d_{min}.

$$d_{\mathrm{min}} = \min_{1 \le k \le n} d\left(\boldsymbol{y}, \boldsymbol{x}_k\right) \tag{22}$$

where $d\left(\boldsymbol{y}, \boldsymbol{x}_k\right)$ represents the distance between $\boldsymbol{y}$ and $\boldsymbol{x}_k$.

By traversing all points in space $\boldsymbol{S}^d$ by unit length, we obtain the upper bound of the minimum distance, which can

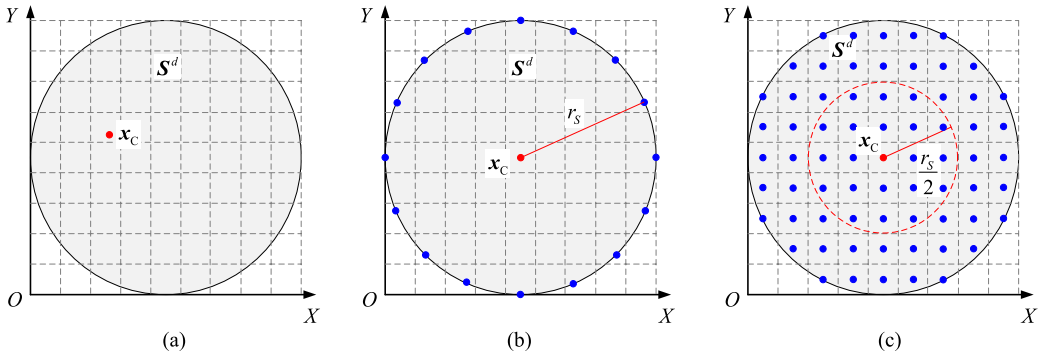

FIGURE 1. A schematic diagram for different values of dispersion in a two-dimensional space. (a) Minimum value of dispersion. (b) Maximum value of dispersion. (c) Constant value of dispersion.

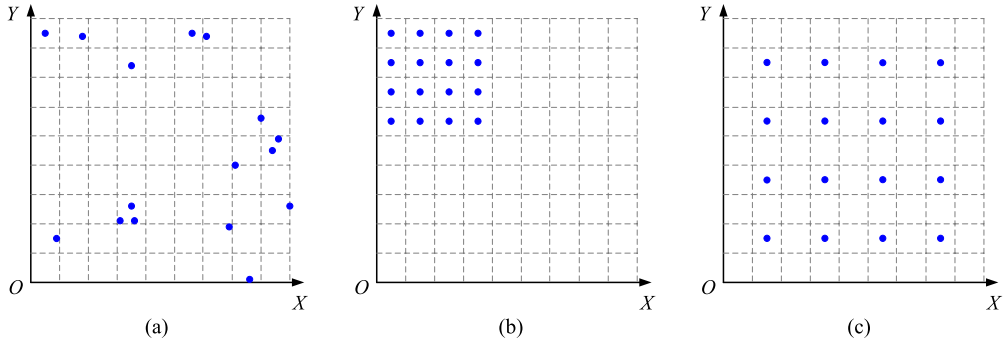

FIGURE 2. A schematic diagram of configurations' spatial distribution in two-dimensional space. (a) Points are dispersive but uneven. (b) Points are concentrated but even. (c) Points are dispersive and even.

be expressed as $d_{\sup}$.

$$d_{\sup} = \sup_{\boldsymbol{y}\in\boldsymbol{S}^d} d_{\min} = \sup_{\boldsymbol{y}\in\boldsymbol{S}^d}\left(\min_{1\le k\le n} d\left(\boldsymbol{y},\boldsymbol{x}_k\right)\right) \tag{23}$$

$d_{\sup}$ can be understood as the radius of the largest sphere that can be accommodated in $\boldsymbol{S}^d$ after removing the space formed by $\boldsymbol{A}$.

Then the evenness of the point set $\boldsymbol{A}$ is

$$U(\boldsymbol{A}) = \frac{d_{\text{ave}}}{d_{\sup}} = \frac{\sqrt{\frac{1}{n}\sum_{i=1}^{n}\left(\boldsymbol{x}_i-\boldsymbol{x}_{\text{C}}\right)^{\text{T}}\left(\boldsymbol{x}_i-\boldsymbol{x}_{\text{C}}\right)}}{\sup\limits_{\boldsymbol{y}\in\boldsymbol{S}^d}\left(\min\limits_{1\le k\le n} d\left(\boldsymbol{y},\boldsymbol{x}_k\right)\right)} \tag{24}$$

The bigger the $U(\boldsymbol{A})$, the better the evenness of the points set $\boldsymbol{A}$.

Then evenness of configurations $\bar{\boldsymbol{\theta}}$ can be calculated as (25), shown at the bottom of the next page, where $\boldsymbol{P}'$ is a random point in manipulator's workspace. We can evaluate configurations' evenness by (25). The bigger the $U(\bar{\boldsymbol{\theta}})$, the better the evenness of configurations.

We can analyze range of evenness by taking a two-dimensional circular workspace (shows in Fig. 1) as an example. The range of the molecular of evenness is $\left[0, \sqrt{r_S}\right]$. When configuration number approaches infinity and end points corresponding to the configurations fill the entire workspace, the molecular of (25) approaches a fixed value $\sqrt{r_S/2}$. The denominator of evenness (25) as configuration number increases, and the minimum value is zero. Therefore, configurations' evenness increases as configuration number increases, and the maximum value is gigantic.

The spatial distribution of end points can intuitively display the configurations' spatial distribution. We take a two-dimensional space as an example; Fig. 2 shows three types of the configurations' spatial distribution.

Fig. 2 shows the dispersive and even configurations can cover workspace best; and we can obtain a set of configurations that have the best globality by using dispersion index and evenness index.

C. COMPREHENSIVE QUALITY INDEX OF CONFIGURATIONS

Since the observability indexes and globality indexes evaluate configurations' quality from different aspects, we need to integrate these indexes.

The first step is to normalize observability indexes and globality indexes because they have different ranges. The most common normalization method is linear transformation method (also known as min-max normalization), which requires ranges of data.

However, linear transformation method is not suitable for our situation, because it is hard to calculate the ranges of the

above indexes. Assuming that each joint angle's range of an n-DOF manipulator is $\pm 180°$, we traverse at intervals of 10° to get $M = 36^n$ configurations. If calibration configuration number is m, then m calibration configurations are selected among M configurations, and the number of the possible situations is $M!/[m!\,(M-m)!]$.We have to calculate the above indexes in all situations to get ranges of the indexes. However, the number of possible situations will be very large when DOF is high, traversal intervals are small, or the calibration configuration number is large. Therefore, it is unrealistic to calculate indexes' ranges. For this reason, this paper uses a normalization method based on inverse tangent function as (26).

$$x_{\text{Norm}} = \frac{2}{\pi} \cdot \arctan(x), \quad \text{if and only if } x > 0. \tag{26}$$

where x_{Norm} is normalized value of x.

This normalization method is a kind of nonlinear normalization method which uses the inverse tangent function to map the original values. The feature of this method guarantees it can avoid a large number of traversal operations in linear transformation, and it is suitable for scenes where data is scattered. Therefore, we choose this method to improve the normalization efficiency. And after transformation of (26), we can map each index into the interval $(-1, 1)$.

Then comprehensive quality index can be calculated as

$$O_C = \frac{2}{\pi}\left(\arctan D + \arctan U + \sum_{i=1}^{3} \arctan O_i\right) \tag{27}$$

This section establishes the observability indexes and globality indexes of calibration configurations. The observability indexes can evaluate the overall observability, average observability, and the worst observability of configurations. The dispersion index and evenness index can evaluate configurations' spatial distribution. By combining the existing observability indexes with dispersion index and evenness index, we proposed a comprehensive quality index (O_C) to evaluate calibration configurations' quality. O_C can simultaneously reflect configurations' observability and globality, so it is more effective than the existing indexes.

IV. CALIBRATION CONFIGURATIONS OPTIMIZATION

To optimize calibration configurations, we establish an optimization model base on the proposed comprehensive quality index and constraints including configuration number and joint angles ranges. Then, we use PSO to solve configuration optimization model.

A. OPTIMIZATION MODEL

The optimization model includes two parts: objective function, and constraints.

1) OBJECTIVE FUNCTION

The optimization objective is the proposed comprehensive quality index, shown in (28).

$$f(\bar{\boldsymbol{\theta}}) = \frac{2}{\pi}\left(\arctan D(\bar{\boldsymbol{\theta}}) + \arctan U(\bar{\boldsymbol{\theta}}) + \sum_{i=1}^{3} \arctan O_i(\bar{\boldsymbol{\theta}})\right) \tag{28}$$

The benefit of using the proposed comprehensive index instead of multiple single indexes (including three observability indexes and two globality indexes) is to avoid the complexity of multi-objective optimization problems.

2) CONSTRAINTS OF OPTIMIZATION

When we optimize calibration configurations, we also need to consider constrains of configuration number and joint angles.

a: CONSTRAINT OF CONFIGURATION NUMBER

We use p parameters to describe relationship between two link coordinate systems. Then kinematic model of an n-DOF manipulator will have $(n+1)\,p$ kinematic parameters when coordinate system of tool is considered. The kinematic calibration equations established by one configuration contains only 6 equations. In order to ensure equations has a unique solution (or a least square solution), the equation number needs to equal or be greater than the number of unknown variables. Therefore, configuration number should satisfy the following inequality.

$$6m \geq (n+1)\,p,\ m \in \boldsymbol{N}_+ \tag{29}$$

where $\boldsymbol{N}_+$ is positive integer.

Then the constraint of configuration number is

$$m \geq \left\lceil \frac{(n+1)\,p}{6} \right\rceil \tag{30}$$

b: CONSTRAINT OF JOINT ANGLES RANGES

Any produced configuration during the optimization process should meet limits of joint angles ranges.

$$\begin{cases} \theta_1 \in [\theta_{1\_\min}, \theta_{1\_\max}] \\ \theta_2 \in [\theta_{2\_\min}, \theta_{2\_\max}] \\ \vdots \\ \theta_n \in [\theta_{n\_\min}, \theta_{n\_\max}] \end{cases} \tag{31}$$

$$U(\bar{\boldsymbol{\theta}}) = \frac{\sqrt{\frac{1}{m}\sum_{i=1}^{m}\left(\boldsymbol{P}_{d\_i}(\boldsymbol{\theta}_i) - \frac{1}{m}\sum_{i=1}^{m}\boldsymbol{P}_{d\_i}(\boldsymbol{\theta}_i)\right)^{\mathrm{T}}\left(\boldsymbol{P}_{d\_i}(\boldsymbol{\theta}_i) - \frac{1}{m}\sum_{i=1}^{m}\boldsymbol{P}_{d\_i}(\boldsymbol{\theta}_i)\right)}}{\sup_{\boldsymbol{P}' \in \Re^3}\left(\min_{1\leq k\leq m} d\left(\boldsymbol{P}', \boldsymbol{P}_{d_k}(\boldsymbol{\theta}_k)\right)\right)} \tag{25}$$

where $\theta_1, \theta_2, \cdots, \theta_n$ are joint angles of the i-th configuration, i.e. $\boldsymbol{\theta}_i = [\theta_1, \theta_2, \cdots, \theta_n]$; and $[\theta\_i_{\min}, \theta\_i_{\max}]$ is joint angle range of i-th joint.

Based on objective function and two types of constraints, we can convert optimization of calibration configurations into the maximization of the comprehensive quality index under the constraints of configuration number and joint angles ranges. If we use $\bar{\boldsymbol{\theta}} = [\boldsymbol{\theta}_1, \boldsymbol{\theta}_2, \cdots, \boldsymbol{\theta}_m]$ represent a configuration set that have m configurations, the above optimization can be described as

$$\begin{aligned} &\max f(\bar{\boldsymbol{\theta}}) = \frac{2}{\pi}\left(\arctan D(\bar{\boldsymbol{\theta}}) + \arctan U(\bar{\boldsymbol{\theta}}) + \sum_{i=1}^{3}\arctan O_i(\bar{\boldsymbol{\theta}})\right) \\ &\text{s.t. } m \geq \left\lceil \frac{(n+1)\,p}{6} \right\rceil \\ &\text{s.t. } \begin{cases} \theta_1 \in [\theta\_1_{\min}, \theta\_1_{\max}] \\ \theta_2 \in [\theta\_2_{\min}, \theta\_2_{\max}] \\ \vdots \\ \theta_n \in [\theta\_n_{\min}, \theta\_n_{\max}] \end{cases} \end{aligned} \tag{32}$$

B. OPTIMIZATION ALGORITHM BASED ON PSO

Based on the optimization model, this paper uses the PSO to optimize calibration configurations.

1) INITIALIZE PARTICLES

When we optimize m configurations for an n-DOF manipulator, dimension of search space (i.e. dimension of particle) is $d = m \cdot n$. Each configuration can be expressed as $\boldsymbol{\theta}_i = \left[\theta_{i\_1}, \theta_{i\_2}, \cdots, \theta_{i\_n}\right] \in \Re^n$, where $i = 1, 2, \cdots, m$. Then decision vector (i.e. a particle) of algorithm is

$$\bar{\boldsymbol{\theta}} = [\boldsymbol{\theta}_1, \boldsymbol{\theta}_2, \cdots, \boldsymbol{\theta}_m] \tag{33}$$

where $\bar{\boldsymbol{\theta}} \in \Re^d$.

Velocity vector of each particle has same dimension as particle, i.e. $\bar{\boldsymbol{v}} \in \Re^d$, and it can be expressed as

$$\bar{\boldsymbol{v}} = [\boldsymbol{v}_1, \boldsymbol{v}_2, \cdots, \boldsymbol{v}_m] \tag{34}$$

where $\boldsymbol{v}_i = \left[v_{i\_1}, v_{i\_2}, \cdots, v_{i\_n}\right]$ is velocity of joint angles of the i-th configuration.

A particle swarm has N_{Swrm} particles; each particle has a structure as in (33), and represents m configurations. Initial value ($\bar{\boldsymbol{\theta}}_{\text{ini}}$) and initial velocity ($\bar{\boldsymbol{v}}_{\text{ini}}$) of each particle is randomly selected within joint angles ranges.

2) FITNESS FUNCTION

Fitness function can be determined by the objective function, as (35).

$$\max f(\bar{\boldsymbol{\theta}}) \frac{2}{\pi}\left(\arctan D(\bar{\boldsymbol{\theta}}) + \arctan U(\bar{\boldsymbol{\theta}}) + \sum_{i=1}^{3}\arctan O_i(\bar{\boldsymbol{\theta}})\right) \tag{35}$$

3) UPDATE PARTICLES' VELOCITY AND POSITION

Assume that optimization needs to be iterated N_{Iter} times. For the j-th ($j = 1, 2, \cdots, N_{\text{Swrm}}$) particle in the k-th ($k = 1, 2, \cdots, N_{\text{Iter}}$) iteration, We use $\bar{\boldsymbol{\theta}}_j^k$ and $\bar{\boldsymbol{v}}_j^k$ represent particle's position and velocity, and use $\boldsymbol{p}_{j\_\text{best}}^k$ and $\boldsymbol{p}_{\text{S\_best}}^k$ represent particle's best-known position and swarm's best-known position. Then particle's position and velocity in next iteration is

$$\begin{cases} \bar{\boldsymbol{v}}_j^{k+1} = \omega\bar{\boldsymbol{v}}_j^k + c_1\sigma\left(\boldsymbol{p}_{j\_\text{best}}^k - \bar{\boldsymbol{\theta}}_j^k\right) + c_2\eta\left(\boldsymbol{p}_{\text{S\_best}}^k - \bar{\boldsymbol{\theta}}_j^k\right) \\ \bar{\boldsymbol{\theta}}_j^{k+1} = \bar{\boldsymbol{\theta}}_j^k + \xi\bar{\boldsymbol{v}}_j^{k+1} \end{cases} \tag{36}$$

where ω determines dependence of particles on initial values, i.e. particles' ability to explore global solution space. σ is randomly distributed on [0, 1], which together with c_1 determines dependence of particle's best-known position. η is randomly distributed on [0, 1], which together with c_2 determines dependence of swarm's best-known position. ξ determines dependence of updated velocity.

ω is linearly decreasing, and the change rule is

$$\omega = \omega_{\max} - \frac{k}{N_{\text{Iter}}}(\omega_{\max} - \omega_{\min}) \tag{37}$$

where $\omega_{\max}$ and $\omega_{\min}$ are upper and lower bond of the ω.

Change rules of c_1 and c_2 is

$$\begin{cases} c_1 = 4 - e^{-\tau\left|\text{mean}\left(O_{\text{C}}(\boldsymbol{p}_1^k), O_{\text{C}}(\boldsymbol{p}_2^k), \cdots, O_{\text{C}}\left(\boldsymbol{p}_q^k\right)\right) - O_{\text{C}}(\boldsymbol{p}_s^k)\right|} \\ c_2 = 4 - c_1 \end{cases} \tag{38}$$

where $\tau = 1$, and mean $(\cdot)$ represents calculating average.

Optimization process continuously updates particle's position and velocity according (36). When every particle's velocity is zero and particle's position no longer changes, or iterations reaches upper bond, optimization complete, and decision vector' s end value is swarm's current best-known position. Then optimized configurations can be obtained by splitting the decision vector into m sub-vectors.

The ideas of this paper can be summarized as follows. Firstly, we analyze factors affecting calibration performance. Secondly, we proposed dispersion index and evenness index of configurations, and combined these indexes with configurations' observability indexes to construct a comprehensive quality index. Finally, we design a configuration optimization algorithm based on PSO. The process of configuration optimization is shown in Fig. 3.

V. SIMULATION

To validate the proposed comprehensive quality index and optimization method, we design four simulations. The first simulation analyzes relationship between configurations' globality index and calibration performance. The second simulation analyzes relationship between comprehensive quality index and calibration performance. The third simulation is to determining configuration number for a specific manipulator. The forth simulation carries out optimization of calibration

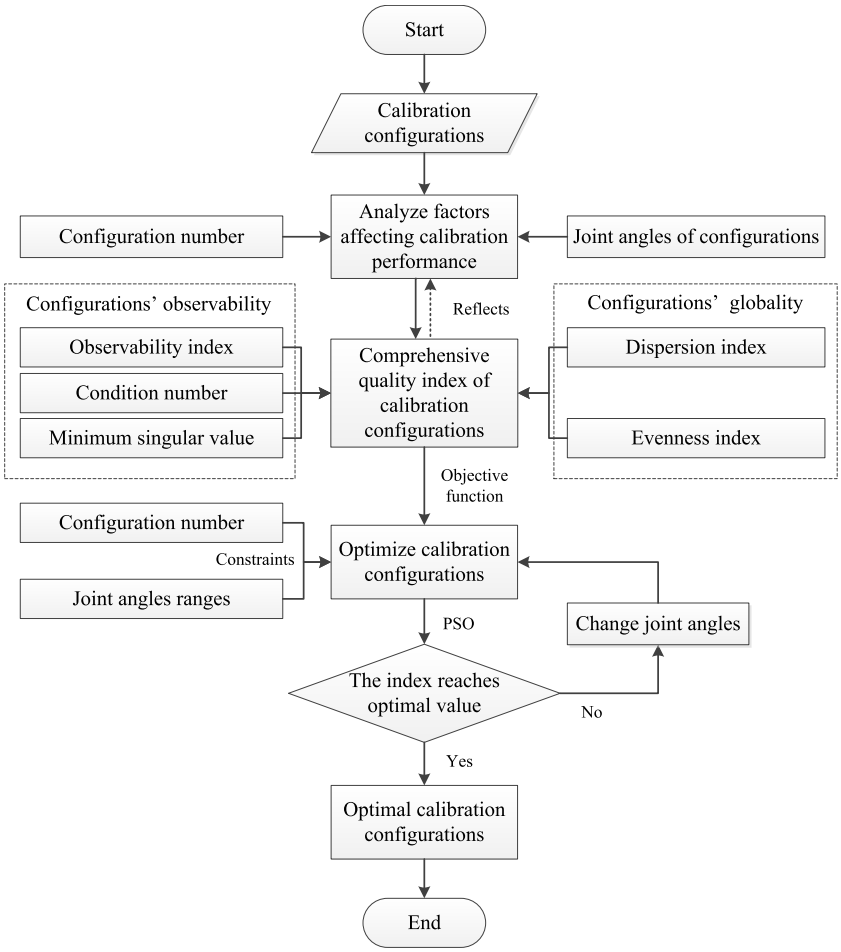

FIGURE 3. Process of calibration configuration optimization.

configurations, and contrasts calibration performance before and after optimization.

A. SUBJECT

The subject of all simulations is an 8-DOF manipulator. Fig. 4 shows the 8-DOF manipulator and its improved Denavit-Hartenberg model [28] with coordinate systems. Table 1 shows kinematic parameters of the 8-DOF manipulator.

TABLE 1. Kinematic parameters of the 8-DOF manipulator.

Link	α(°)	a(mm)	θ(°)	d(mm)	β(°)
1	0	0	90	385	0
2	-90	0	-90	110	0
3	90	0	0	245	0
4	0	135	0	0	0
5	0	135	-90	0	0
6	-90	0	0	300	0
7	90	0	0	0	0
8	-90	0	0	93	0
E	0	0	0	140	0

The meaning of the kinematic parameters mentioned in Table I is showed in Appendix. In particular, the improved Denavit-Hartenberg model adds an angle β for describing the rotation of the adjacent joints' axis about the y-axis based on the classical D-H model. Adding this parameter can eliminate the mutation of parameters of adjacent parallel joints.

B. INFLUENCE OF CONFIGURATIONS' QUALITY INDEXES ON CALIBRATION

In this section, we will simulate influences of globality indexes and comprehensive quality index on calibration.

1) INFLUENCE OF CONFIGURATIONS' GLOBALITY INDEXES ON CALIBRATION

We carry out the following simulation to show influence of configurations' globality indexes on calibration. We randomly generate two sets of configurations with different globalities. Each set contains 30 configurations. Fig. 5 and Fig. 6 show distribution of end position points of two configuration sets. Configuration set A is more concentrated in one area of workspace, while configuration set B covers workspace better.

Table 2 shows dispersion index and evenness index of two configuration sets. We can see that dispersion index and evenness index for the configuration set with better coverage of workspace are both higher.

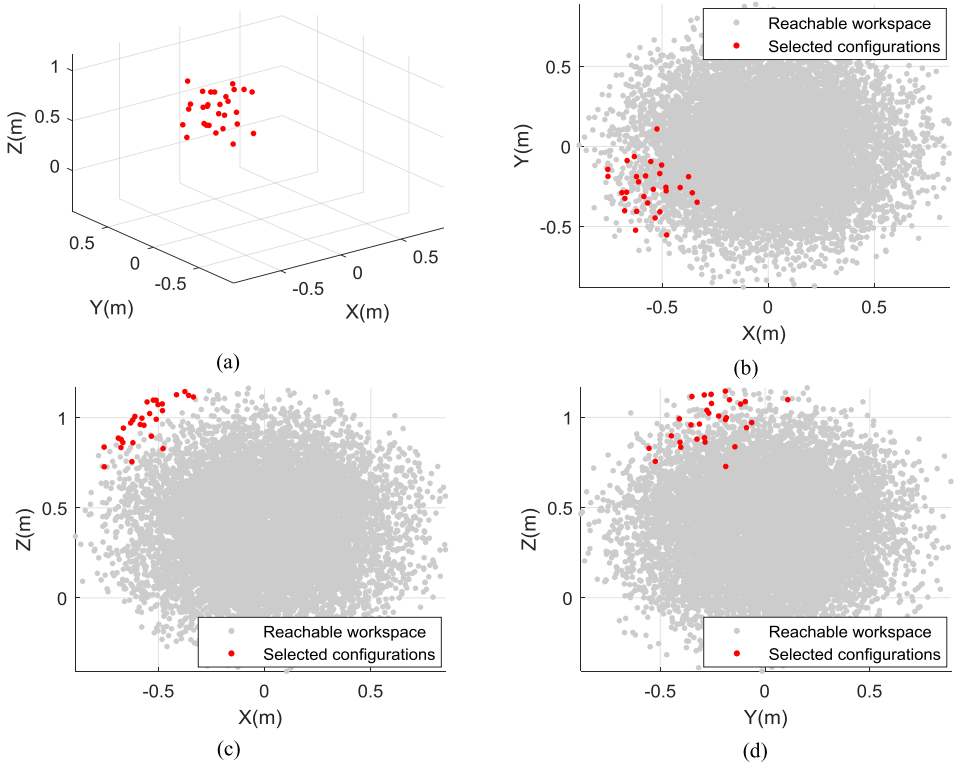

FIGURE 5. Distribution of end points of configuration set A in workspace. (a) 3D View. (b) Points projection on the XOY plane. (c) Points projection on the XOZ plane. (d) Points projection on the YOZ plane.

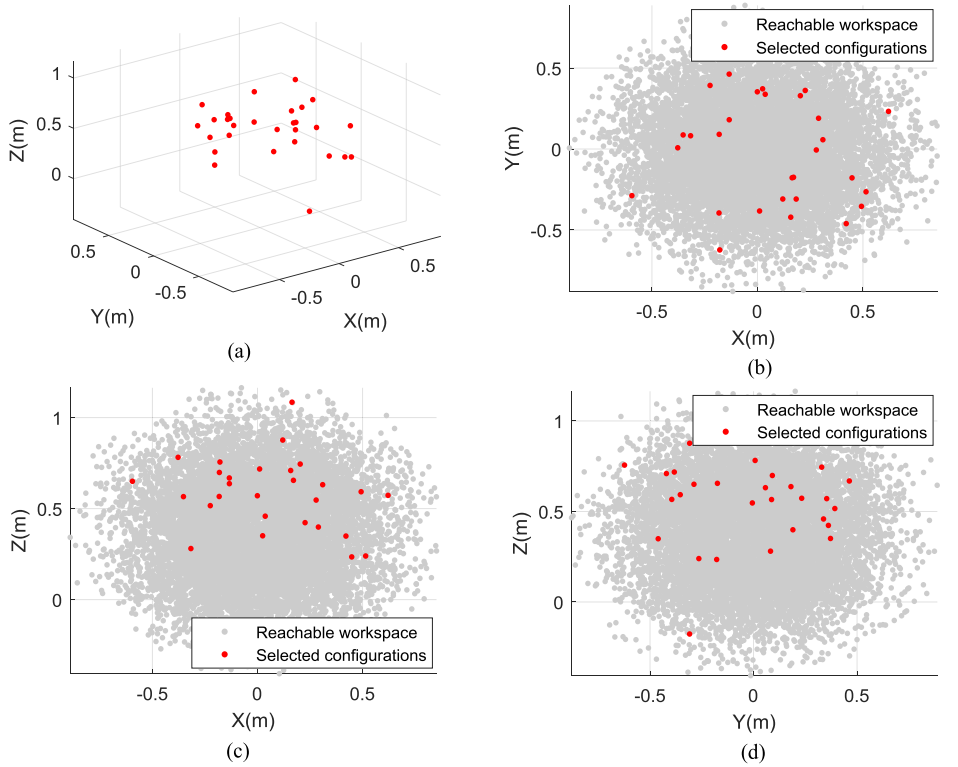

FIGURE 6. Distribution of end points of configuration set B in workspace. (a) 3D View. (b) Points projection on the XOY plane. (c) Points projection on the XOZ plane. (d) Points projection on the YOZ plane.

Two kinematic calibration simulations are carried out using configuration set A and configuration set B respectively. In both of the simulations, range of kinematic parameter errors is set to ± 30mm and $\pm 1.72°$, and measurement error

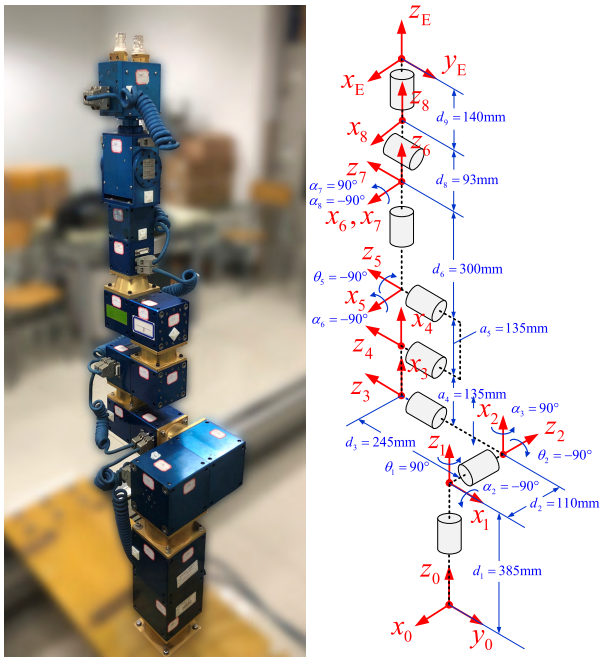

FIGURE 4. 8-DOF manipulator and its coordinate systems.

TABLE 2. Configurations' globality indexes of two configuration sets.

Configuration sets	Dispersion index	Evenness index
Set A	0.04566	0.12536
Set B	0.19232	0.38087

is set to ±2mm. 30 configurations are randomly selected as a control group to verify calibration performance. Fig. 7 and Table 3 show comparison of calibration residuals using configurations with different globalities.

TABLE 3. Comparison of calibration residuals using configurations with different globalities.

		End position errors (mm)			End attitude errors (°)		
		Max	Min	Ave	Max	Min	Ave
Before calibration		148.20	13.65	65.40	24.61	1.03	5.50
After calibration	Set A	21.14	3.60	11.41	1.41	0.19	0.55
	Set B	2.28	0.45	1.38	0.27	0.02	0.10

'Max' is the short form of 'Maximum', 'Min' is the short form of 'Minimum', 'Ave' is the short form of 'Average'.

'Max' is the short form of 'Maximum', 'Min' is the short form of 'Minimum', 'Ave' is the short form of 'Average'.

Table 3 shows that using configuration set A can reduce average position error by 82.55%, while using configuration set B can reduce average position error by 97.89%. Using configuration set A can reduce average attitude error by 90.00%, while using configuration set B can reduce average attitude error by 98.18%. The results show that under the same calibration conditions (same manipulator, same measurement errors, and same calibration configuration number), using configurations with better globality can improve calibration performance.

2) INFLUENCE OF COMPREHENSIVE QUALITY INDEX ON CALIBRATION

We carry out the following simulation to show the influence of the proposed comprehensive quality index (O_C) on calibration.

We use multiple sets of configurations with different comprehensive quality to calibrate the manipulator, and each set contains 30 configurations. In order to obtain multiple sets of configurations with different O_C, we take the following method. We randomly generate multiple sets of configurations in different joint angles ranges. Joint angles ranges are gradually increased from ±10° to ±180° (the interval is 1°). Then, we calculate the O_C of each configuration set and sort them in the order of small to large. Then, we can get 171 configuration sets with increasing O_C.

We use the 171 configuration sets to calibrate manipulator, and for each calibration, the range of kinematics parameter errors is set to ±30mm and ±1.72°, and the measurement error is set to ±2mm. Extra 30 configurations are randomly selected as a control group to verify the calibration performance. Fig. 8 shows relationship between average calibration residuals of the verification group and O_C.

By analyzing the data, we notice that as O_C increases, calibration residuals gradually decrease, and the downward trend tend to be slow. When O_C increases from the initial 0.0192 to 1.1770, end position error reduces from 98.23mm to 1.32mm, and the position accuracy is improved by 98.68%; end attitude error reduces from 15.84° to 0.04°, and the attitude accuracy is improved by 99.75%. The results show that calibration performance is positively related to O_C. In other word, configurations with higher comprehensive quality index can obtain a better calibration performance.

C. SIMULATION OF CALIBRATION CONFIGURATION OPTIMIZATION

In this section, we will determine the most suitable configuration number for calibration, optimize calibration configurations, and use the optimal configurations to calibrate the 8-DOF manipulator.

1) DETERMINING CONFIGURATION NUMBER FOR CALIBRATION

Too few configurations are not enough to complete calibration, while too many configurations will increase the cost of calibration. Therefore, it is very important to choose an appropriate number of calibration configurations.

a: INFLUENCE OF CONFIGURATION NUMBER ON THE INDEXES

We use numerical methods to analyze relationship between configuration number and configurations' quality indexes.

The above Table 1 shows that kinematic model of the 8-DOF manipulator has 45 kinematic parameters. From (30)

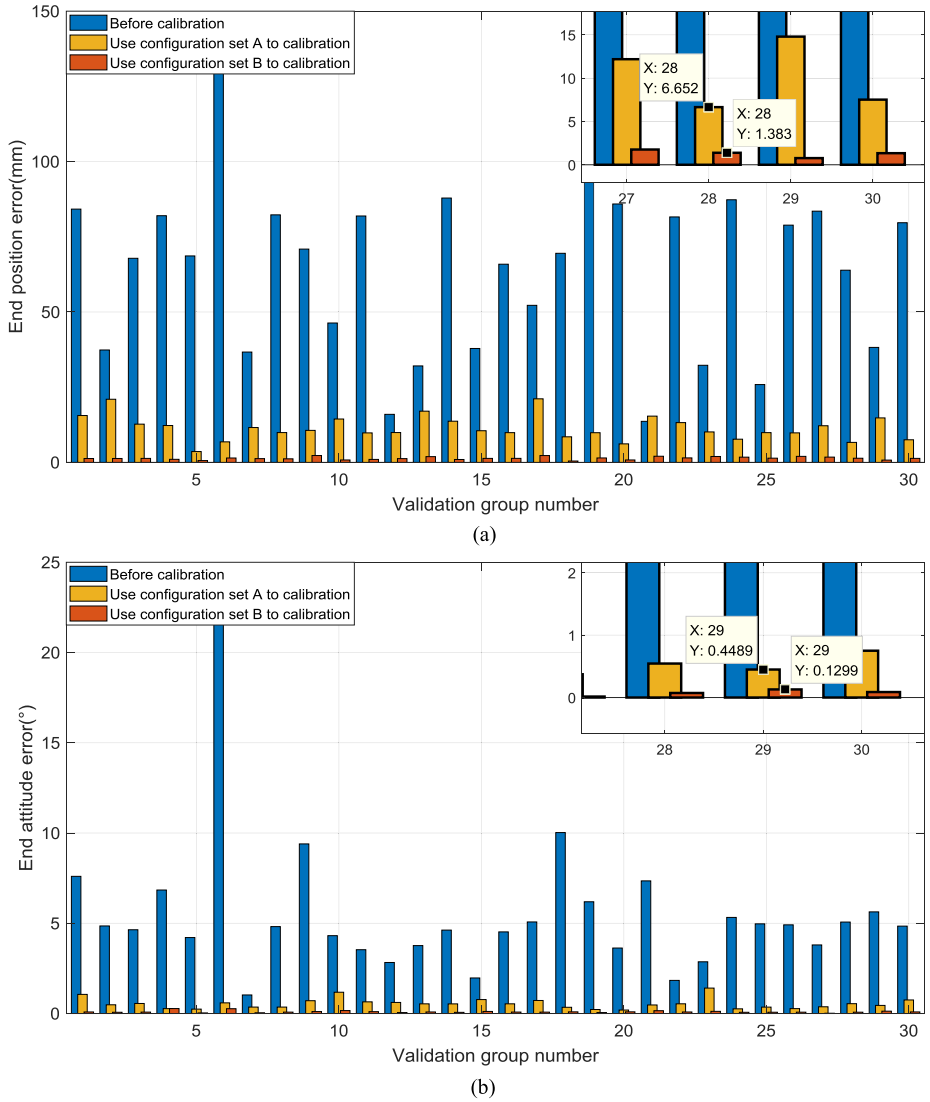

FIGURE 7. Comparison of calibration residuals using configurations with different globalities. (a) End position errors. (b) End attitude errors.

we know that the minimum number of calibration configurations is 8. Therefore, we calculate the four indexes (including the existing indexes O_1, O_2, O_3, and the proposed index O_C in this paper) when calibration number increasing from 8 to 500.

Fig. 9 shows relationship between configuration number and indexes. By analyzing the data, we notice that as configuration number increases, values of the indexes increase gradually, and the upward trend tend to be slow.

We can analyze the data with O_C as an example. O_C increases by 103.21% when configuration number increase from 8 to 50. This situation indicates that the increase in configuration number in the interval [8, 50] significantly improves quality of configuration set. O_C increases by 16.49% when configuration number increase from 50 to 100. This situation indicates that cost of upgrading the quality of configuration set is gradually increasing. O_C increases by 27.98% when configuration number increase from 100 to 500. This situation indicates that the increase in configuration number in the interval [100, 500] has slightly improved quality of configuration set.

Fig. 10 shows O_C's growth trend with configuration number. By analyzing the data, we notice that when configuration number increases to more than 40, gradient of O_C begins to decrease; when configuration number increases to more than 120, the increase in configuration number only improve the quality of configuration set slightly.

b: INFLUENCE OF CONFIGURATION NUMBER ON CALIBRATION PERFORMANCE

We use numerical methods to analyze relationship between configuration number and calibration performance. We use multiple sets of configurations with different configuration number to calibration. For each calibration, we randomly generate configurations, and configuration number increases

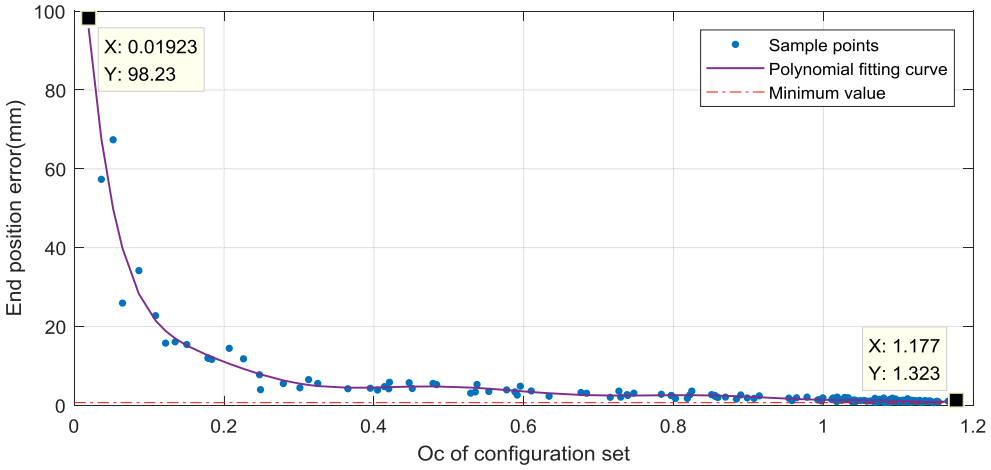

(a)

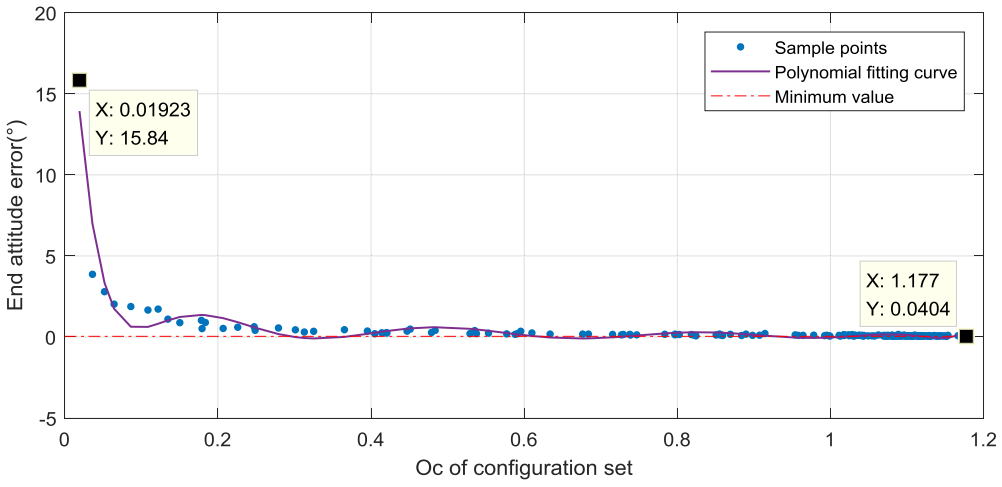

(b)

FIGURE 8. Relationship between calibration residuals and O_C. (a) End position errors. (b) End attitude errors.

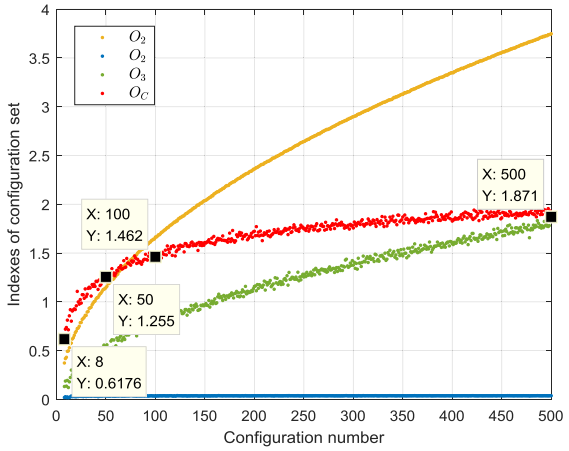

FIGURE 9. Relationship between configuration number and the indexes.

from 8 to 200. Range of kinematic parameter errors is set to ±30mm and ±1.72°, and measurement error is set to ±2mm.

We calculate calibration residuals after each calibration, and use polynomials to fit the data. Fig. 11 shows relationship between calibration residuals and configuration number.

By analyzing the data, we notice that as configuration number increases, calibration residuals gradually decrease, and the downward trend tend to be slow. Table 4 shows calibration performance when configuration number is 8, 20, 60, and 200.

Results in Fig. 11 and Table 4 show that excessive configurations are not beneficial to improve calibration performance effectively.

TABLE 4. Calibration performance when configuration number is 8, 20, 60, and 200.

Configuration number	End position error	Compared with the situation of 8 configurations	End attitude error	Compared with the situation of 8 configurations
8	2.56mm	-	0.22°	-
20	1.20mm	53.13% lower	0.07°	68.18% lower
60	0.60mm	76.56% lower	0.04°	81.82% lower
200	0.35mm	86.33% lower	0.02°	90.91% lower

The above subsections consider the factors including comprehensive quality index, calibration performance,

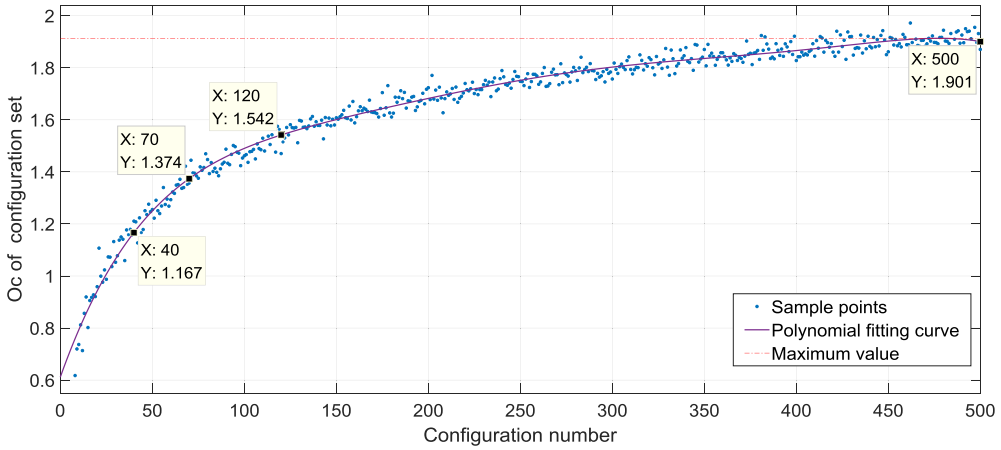

FIGURE 10. Relationship between configuration number and O_C.

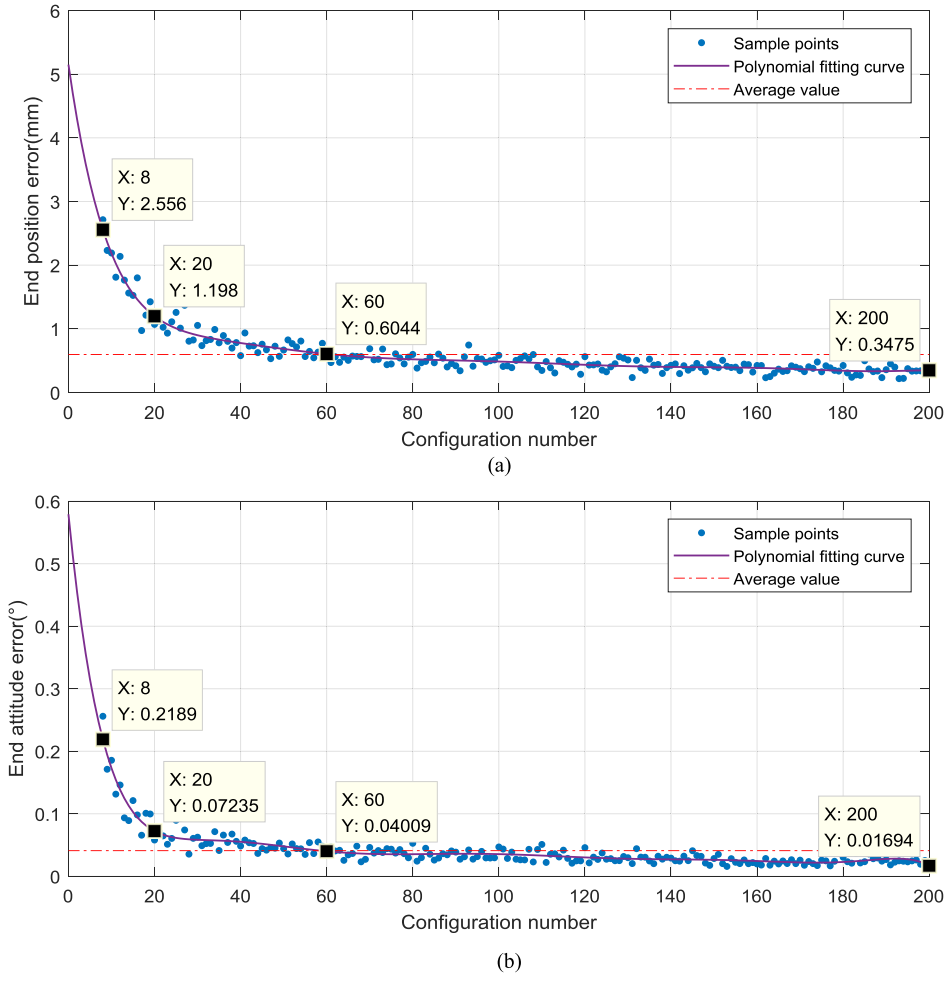

FIGURE 11. Relationship between configuration number and calibration residuals. (a) End position errors. (b) End attitude errors.

and calibration efficiency. Simulation results show that for the 8-DOF manipulator shown in Fig. 4, the suitable range of calibration configuration number is 40 to 60.

2) OPTIMIZATION SIMULATION OF CALIBRATION CONFIGURATIONS BASED ON PSO

Based on the determined configuration number range in the previous section, we choose 40 as calibration

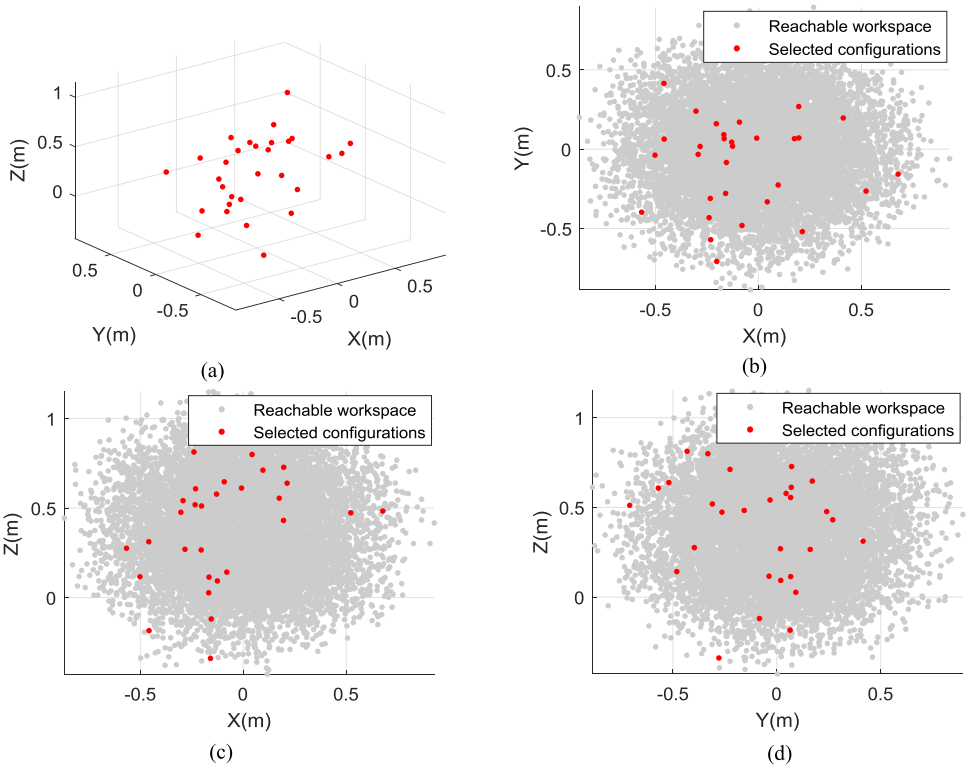

FIGURE 12. Distribution of end points of optimal configuration set. (a) 3D View. (b) Points projection on the XOY plane. (c) Points projection on the XOZ plane. (d) Points projection on the YOZ plane.

configuration number. Particles can be initialized by (33), and dimension of search space is $d = 320$. Table 5 shows parameters of configuration optimization algorithm based on PSO.

TABLE 5. Parameters of PSO algorithm for configuration optimization.

Parameter	Change rule	Value / Range
N_{Swrm}	—	20
N_{Iter}	—	200
ξ	—	0.729
ω	Linear decrement	[0.4,0.95]
c_1	Decrement	(0,4)
c_2	Decrement	(0,4)

After optimization, O_C of the optimal configuration set is 1.4259. Fig. 12 shows distribution of the end points of optimal configuration set.

In the following sections we will use multiple random configuration sets as control groups, and contrast configurations' dispersion index, evenness index, comprehensive quality index, and calibration performance before and after optimization.

a: COMPARISON OF CONFIGURATIONS' QUALITY BEFORE AND AFTER OPTIMIZATION

We randomly generate 500 configuration sets; each configuration set has 40 configurations. Fig. 13, Fig. 14, and Fig. 15 shows comparison of configurations' dispersion index, evenness index, and comprehensive quality index, respectively.

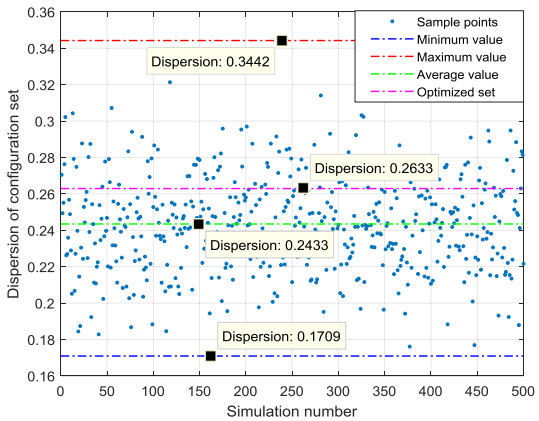

FIGURE 13. Comparison of configurations' dispersion index.

Table 6 shows comparison of indexes of random configuration set and optimal configuration set. The dispersion index, evenness index, and comprehensive quality index of optimal configuration set are all higher than average value of these indexes of the random configuration sets. Therefore, quality of optimal set is better than random set.

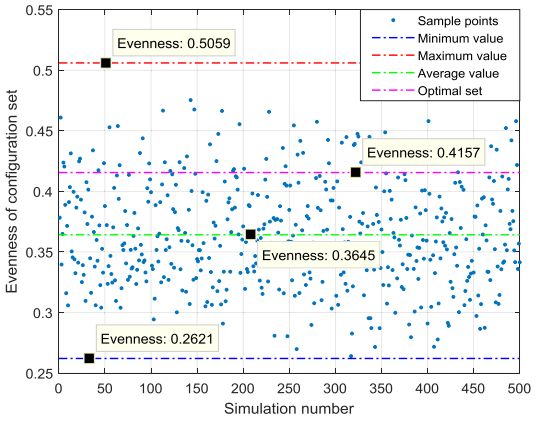

FIGURE 14. Comparison of configurations' evenness index.

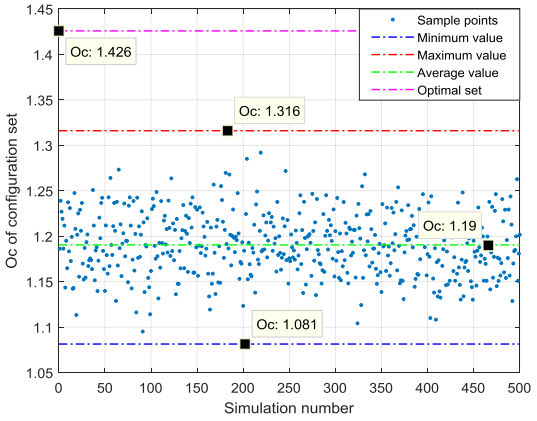

FIGURE 15. Comparison of configurations' comprehensive quality index.

TABLE 6. Comparison of indexes of random configuration set and optimal configuration set.

Configuration set	Dispersion index	Evenness index	Comprehensive quality index
Random set	0.2433 (average)	0.3645 (average)	1.1900 (average)
Optimal set	0.2633	0.4157	1.4259

b: COMPARISON OF CALIBRATION PERFORMANCE BEFORE AND AFTER CONFIGURATION OPTIMIZATION

We use random configurations and optimal configurations to carry out 100 calibration simulations. For each calibration, range of kinematics parameter errors is set to $\pm$30mm and $\pm$1.72°, and measurement error is set to $\pm$2mm. Fig. 16 shows calibration residuals. Table 7 shows comparison of the calibration performance by using random configurations and optimal configurations. By analyzing the data, we notice that calibration performance is improved by using optimal configurations, and the improvement of position accuracy is more obvious.

Through the above simulations, we draw the following conclusions:

- Those configurations that cover manipulator's workspace better have better globality. Configurations that have a higher comprehensive quality index can obtain a higher calibration performance.
- Comprehensive quality index and calibration performance both increase as configuration number increases, but the growth trends of both are slow down. Considering the effect of configuration number on calibration efficiency, we believe that too many configurations are not beneficial to calibration.
- The proposed method in this paper can optimize configurations' observability and globality. Calibration performance is improved by using optimal configurations, with the position accuracy increased by 43.86% and the attitude accuracy increased by 14.29%.

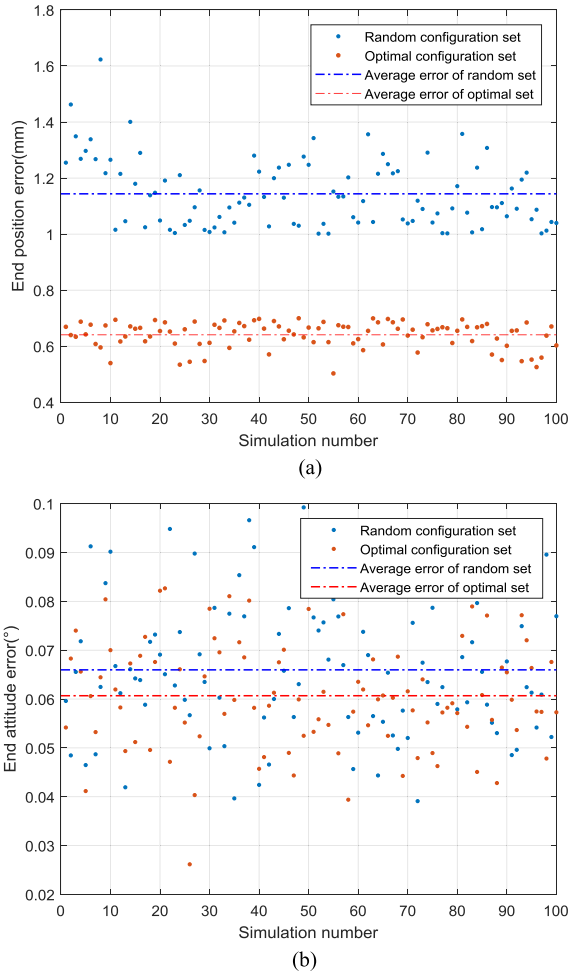

FIGURE 16. Calibration residuals using random configurations and optimal configurations. (a) End position errors. (b) End attitude errors.

TABLE 7. Compare calibration performance of random configurations and optimal configurations.

Configuration set	End position error		End attitude error	
	Ave	Max	Ave	Max
Random set	1.14mm	1.62mm	0.07°	0.10°
Optimal set	0.64mm (43.86% lower)	0.70mm (56.79% lower)	0.06° (14.29% lower)	0.09° (10.00% lower)

VI. CONCLUSION

To improve manipulator's calibration performance, this paper carries out a configuration optimization method. We analyzed

factors affecting calibration performance, and used statistical theory to establish comprehensive quality index of calibration configurations. Then, we used numerical methods to analyze relationships between comprehensive quality index and configuration number, calibration accuracy and configuration number, and we gained a suitable range of configuration number. Furthermore, we established a configuration optimization model based on the comprehensive quality index, and constraints of configuration number and joint angles ranges. PSO was used to solve configuration optimization model. To validate our method, we used an 8-DOF manipulator for simulation. The result showed that configurations optimized by the proposed method can effectively improve calibration performance.

The contributions of this paper mainly include the following points:

- We established configurations' dispersion index and evenness index by considering the distribution of a manipulator's end points in workspace. These indexes can be used to obtain configurations with a better globality.
- By combining the existing observability indexes with globality indexes, we proposed a comprehensive quality index, which can simultaneously reflect calibration configurations' observability and globality.
- Numerical methods were used to analyze relationships between comprehensive quality index and configuration number, calibration accuracy and configuration number. Based on the relationships, we provided a feasible solution for determining calibration configuration number for a specific manipulator.

The configuration optimization method proposed in this paper can effectively optimize calibration configurations and improve calibration performance. This method is suitable not only for industrial manipulators, but also for manipulators in space engineering, biomedical, etc. However, when designing the configuration optimization method, this paper only considers constraints of configuration number and joint angles ranges. Problems such as collision between manipulator and environment and measurability of configurations in actual calibration process need further study.

APPENDIX A
KINEMATIC MODEL

The manipulator's kinematic model is established by the improved Denavit-Hartenberg method. This method uses five parameters to represent the homogeneous transformation matrix of two adjacent coordinate systems, as follows

$$ {}^{i-1}_{i}\boldsymbol{T} = \mathrm{Rot}\,(x,\alpha_i)\,\mathrm{Trans}\,(x,a_i)\,\mathrm{Rot}\,(z,\theta_i) \\ \mathrm{Trans}\,(z,d_i)\,\mathrm{Rot}\,(y,\beta_i) \quad (39) $$

where ${}^{i-1}_{i}\boldsymbol{T}$ is the homogeneous transformation matrix between coordinate systems Σ_{i-1} and Σ_i, $\mathrm{Rot}\,(k,\gamma)$ means to rotate γ around the k-axis, $\mathrm{Trans}\,(k,l)$ means to translate l along k-axis. α is the angle at which the coordinate system rotates around the x-axis, a is the distance the coordinate system translates along the x-axis, θ is the angle at which the coordinate system rotates around the z-axis, d is the distance the coordinate system translates along the z-axis, β is the angle at which the coordinate system rotates around the y-axis.

For an n-DOF manipulator, the transformation matrix between base coordinate system and end coordinate system is

$$ {}^{0}_{\mathrm{E}}\boldsymbol{T} = {}^{0}_{1}\boldsymbol{T}\,{}^{1}_{2}\boldsymbol{T}\cdots{}^{n}_{\mathrm{E}}\boldsymbol{T} \quad (40) $$

APPENDIX B
KINEMATIC ERROR MODEL

We use ${}^{i-1}_{i}\boldsymbol{T}$ and ${}^{i-1}_{i}\boldsymbol{T}'$ represent the nominal transformation matrix and the actual transformation matrix respectively. The differential motion between ${}^{i-1}_{i}\boldsymbol{T}$ and ${}^{i-1}_{i}\boldsymbol{T}'$ is

$$ \mathrm{d}\boldsymbol{T}_i = {}^{i-1}_{i}\boldsymbol{T}' - {}^{i-1}_{i}\boldsymbol{T} = {}^{i-1}_{i}\boldsymbol{T}\cdot\boldsymbol{\Delta}_i \quad (i=0,1,2,\cdots) \quad (41) $$

$\boldsymbol{\Delta}_i$ in (42) is the position/attitude error matrix, and it can be represented as

$$ \boldsymbol{\Delta}_i = \begin{bmatrix} 0 & -\delta_{iz} & \delta_{iy} & d_{ix} \\ \delta_{iz} & 0 & -\delta_{ix} & d_{iy} \\ -\delta_{iy} & \delta_{ix} & 0 & d_{iz} \\ 0 & 0 & 0 & 0 \end{bmatrix} \quad (42) $$

where $\boldsymbol{\delta}_i = \begin{bmatrix}\delta_{ix} & \delta_{iy} & \delta_{iz}\end{bmatrix}^{\mathrm{T}}$ and $\boldsymbol{d}_i = \begin{bmatrix}d_{ix} & d_{iy} & d_{iz}\end{bmatrix}^{\mathrm{T}}$ represent position error and attitude error respectively.

$\mathrm{d}\boldsymbol{T}_i$ in (43) can also be approximated as

$$ \mathrm{d}\boldsymbol{T}_i = \frac{\partial^{i-1}_{i}\boldsymbol{T}}{\partial\alpha_i}\Delta\alpha_i + \frac{\partial^{i-1}_{i}\boldsymbol{T}}{\partial a_i}\Delta a_i + \frac{\partial^{i-1}_{i}\boldsymbol{T}_i}{\partial\theta_i}\Delta\theta_i \\ + \frac{\partial^{i-1}_{i}\boldsymbol{T}}{\partial d_i}\Delta d_i + \frac{\partial^{i-1}_{i}\boldsymbol{T}}{\partial\beta_i}\Delta\beta_i \quad (43) $$

The position/attitude error model of the adjacent link coordinate systems shown in (44) can be derived by (39), (42), and (43),

$$ \begin{bmatrix} d_{ix} \\ d_{iy} \\ d_{iz} \\ \delta_{ix} \\ \delta_{iy} \\ \delta_{iz} \end{bmatrix} = \begin{bmatrix} \boldsymbol{k}_i^1 & \boldsymbol{k}_i^2 & \boldsymbol{k}_i^3 & \boldsymbol{k}_i^4 & \boldsymbol{k}_i^5 \\ \boldsymbol{k}_i^6 & \boldsymbol{k}_i^7 & \boldsymbol{k}_i^8 & \boldsymbol{k}_i^9 & \boldsymbol{k}_i^{10} \end{bmatrix} \begin{bmatrix} \Delta\alpha_i \\ \Delta a_i \\ \Delta\theta_i \\ \Delta d_i \\ \Delta\beta_i \end{bmatrix} \quad (44) $$

where,

$$ \boldsymbol{k}_i^1 = \begin{bmatrix} -d_i\mathrm{s}\theta_i\mathrm{c}\beta_i \\ -d_i\mathrm{c}\theta_i \\ -d_i\mathrm{s}\theta_i\mathrm{s}\beta_i \end{bmatrix}, \quad \boldsymbol{k}_i^2 = \begin{bmatrix} \mathrm{c}\theta_i\mathrm{c}\beta_i \\ -\mathrm{s}\theta_i \\ \mathrm{c}\theta_i\mathrm{s}\beta_i \end{bmatrix}, \boldsymbol{k}_i^3 = \begin{bmatrix} 0 \\ 0 \\ 0 \end{bmatrix}, $$

$$ \boldsymbol{k}_i^4 = \begin{bmatrix} -\mathrm{s}\beta_i \\ 0 \\ \mathrm{c}\beta_i \end{bmatrix}, \quad \boldsymbol{k}_i^5 = \begin{bmatrix} 0 \\ 0 \\ 0 \end{bmatrix}, \boldsymbol{k}_i^6 = \begin{bmatrix} \mathrm{c}\theta_i\mathrm{c}\beta_i \\ -\mathrm{s}\theta_i \\ \mathrm{c}\theta_i\mathrm{s}\beta_i \end{bmatrix}, $$

$$ \boldsymbol{k}_i^7 = \begin{bmatrix} 0 \\ 0 \\ 0 \end{bmatrix}, \quad \boldsymbol{k}_i^8 = \begin{bmatrix} -\mathrm{s}\beta_i \\ 0 \\ \mathrm{c}\beta_i \end{bmatrix}, \boldsymbol{k}_i^9 = \begin{bmatrix} 0 \\ 0 \\ 0 \end{bmatrix}, \boldsymbol{k}_i^{10} = \begin{bmatrix} 0 \\ 1 \\ 0 \end{bmatrix}. $$

We use ${}^{0}_{\mathrm{E}}\boldsymbol{T}$ and ${}^{0}_{\mathrm{E}}\boldsymbol{T}'$ represent the nominal transformation matrix and the actual transformation matrix between end

$$\boldsymbol{D} = \sum_{i=1}^{n+1} \begin{bmatrix} (\boldsymbol{n}_{i+1}^u)^{\mathrm{T}}\boldsymbol{k}_i^1 + (\boldsymbol{p}_{i+1}^u \times \boldsymbol{n}_{i+1}^u)^{\mathrm{T}}\boldsymbol{k}_i^6 & (\boldsymbol{n}_{i+1}^u)^{\mathrm{T}}\boldsymbol{k}_i^2 & (\boldsymbol{p}_{i+1}^u \times \boldsymbol{n}_{i+1}^u)^{\mathrm{T}}\boldsymbol{k}_i^8 & (\boldsymbol{n}_{i+1}^u)^{\mathrm{T}}\boldsymbol{k}_i^4 & (\boldsymbol{p}_{i+1}^u \times \boldsymbol{n}_{i+1}^u)^{\mathrm{T}}\boldsymbol{k}_i^{10} \\ (\boldsymbol{o}_{i+1}^u)^{\mathrm{T}}\boldsymbol{k}_i^1 + (\boldsymbol{p}_{i+1}^u \times \boldsymbol{o}_{i+1}^u)^{\mathrm{T}}\boldsymbol{k}_i^6 & (\boldsymbol{o}_{i+1}^u)^{\mathrm{T}}\boldsymbol{k}_i^2 & (\boldsymbol{p}_{i+1}^u \times \boldsymbol{o}_{i+1}^u)^{\mathrm{T}}\boldsymbol{k}_i^8 & (\boldsymbol{o}_{i+1}^u)^{\mathrm{T}}\boldsymbol{k}_i^4 & (\boldsymbol{p}_{i+1}^u \times \boldsymbol{o}_{i+1}^u)^{\mathrm{T}}\boldsymbol{k}_i^{10} \\ (\boldsymbol{a}_{i+1}^u)^{\mathrm{T}}\boldsymbol{k}_i^1 + (\boldsymbol{p}_{i+1}^u \times \boldsymbol{a}_{i+1}^u)^{\mathrm{T}}\boldsymbol{k}_i^6 & (\boldsymbol{a}_{i+1}^u)^{\mathrm{T}}\boldsymbol{k}_i^2 & (\boldsymbol{p}_{i+1}^u \times \boldsymbol{a}_{i+1}^u)^{\mathrm{T}}\boldsymbol{k}_i^8 & (\boldsymbol{a}_{i+1}^u)^{\mathrm{T}}\boldsymbol{k}_i^4 & (\boldsymbol{p}_{i+1}^u \times \boldsymbol{a}_{i+1}^u)^{\mathrm{T}}\boldsymbol{k}_i^{10} \\ (\boldsymbol{n}_{i+1}^u)^{\mathrm{T}}\boldsymbol{k}_i^6 & 0 & (\boldsymbol{n}_{i+1}^u)^{\mathrm{T}}\boldsymbol{k}_i^8 & 0 & (\boldsymbol{n}_{i+1}^u)^{\mathrm{T}}\boldsymbol{k}_i^{10} \\ (\boldsymbol{o}_{i+1}^u)^{\mathrm{T}}\boldsymbol{k}_i^6 & 0 & (\boldsymbol{o}_{i+1}^u)^{\mathrm{T}}\boldsymbol{k}_i^8 & 0 & (\boldsymbol{o}_{i+1}^u)^{\mathrm{T}}\boldsymbol{k}_i^{10} \\ (\boldsymbol{a}_{i+1}^u)^{\mathrm{T}}\boldsymbol{k}_i^6 & 0 & (\boldsymbol{a}_{i+1}^u)^{\mathrm{T}}\boldsymbol{k}_i^8 & 0 & (\boldsymbol{a}_{i+1}^u)^{\mathrm{T}}\boldsymbol{k}_i^{10} \end{bmatrix} \begin{bmatrix} \Delta\alpha_i \\ \Delta a_i \\ \Delta\theta_i \\ \Delta d_i \\ \Delta\beta_i \end{bmatrix}$$
$$= \sum_{i=1}^{n+1} \boldsymbol{J}_i \cdot \boldsymbol{e}_i = \boldsymbol{J} \cdot \boldsymbol{e} \tag{52}$$

coordinate system and base coordinate system respectively. Then the differential motion between ${}^0_{\mathrm{E}}\boldsymbol{T}$ and ${}^0_{\mathrm{E}}\boldsymbol{T}'$ is

$${}^0_{\mathrm{E}}\boldsymbol{T}' = {}^0_{\mathrm{E}}\boldsymbol{T} + \mathrm{d}\boldsymbol{T} \tag{45}$$

Bring (40) into (45) and ignore the high order terms, we can get

$$\begin{aligned} {}^0_{\mathrm{E}}\boldsymbol{T}' &= \prod_{i=1}^{n+1} {}^{i-1}_{i}\boldsymbol{T}' = \prod_{i=1}^{n+1} \left({}^{i-1}_{i}\boldsymbol{T} + \mathrm{d}\boldsymbol{T}_i\right) \\ &\approx {}^0_{\mathrm{E}}\boldsymbol{T} + \sum_{i=1}^{n+1} \left(\prod_{j=1}^{i-1} {}^{j-1}_{j}\boldsymbol{T}\right) \cdot \mathrm{d}\boldsymbol{T}_i \cdot \left(\prod_{j=i+1}^{n+1} {}^{j-1}_{j}\boldsymbol{T}\right) \end{aligned} \tag{46}$$

Bring (41) into (46),

$$\begin{aligned} \mathrm{d}\boldsymbol{T} &= \sum_{i=1}^{n+1} \left(\prod_{j=1}^{i-1} {}^{j-1}_{j}\boldsymbol{T}\right) \cdot \mathrm{d}\boldsymbol{T}_i \cdot \left(\prod_{j=i+1}^{n+1} {}^{j-1}_{j}\boldsymbol{T}\right) \\ &= \sum_{i=1}^{n+1} {}^0_{\mathrm{E}}\boldsymbol{T} \cdot \left(\prod_{j=i+1}^{n+1} {}^{j-1}_{j}\boldsymbol{T}\right)^{-1} \cdot \boldsymbol{\Delta}_i \cdot \left(\prod_{j=i+1}^{n+1} {}^{j-1}_{j}\boldsymbol{T}\right) \end{aligned} \tag{47}$$

Rewritten (47),

$$\begin{aligned} \mathrm{d}\boldsymbol{T} &= {}^0_{\mathrm{E}}\boldsymbol{T} \cdot \sum_{i=1}^{n+1} \left(\prod_{j=i+1}^{n+1} {}^{j-1}_{j}\boldsymbol{T}\right)^{-1} \cdot \boldsymbol{\Delta}_i \cdot \left(\prod_{j=i+1}^{n+1} {}^{j-1}_{j}\boldsymbol{T}\right) \\ &= {}^0_{\mathrm{E}}\boldsymbol{T} \cdot \boldsymbol{\Delta} \end{aligned} \tag{48}$$

Then position/attitude error matrix of Σ_{E} is

$$\boldsymbol{\Delta} = \sum_{i=1}^{n+1} \left(\prod_{j=i+1}^{n+1} {}^{j-1}_{j}\boldsymbol{T}\right)^{-1} \cdot \boldsymbol{\Delta}_i \cdot \left(\prod_{j=i+1}^{n+1} {}^{j-1}_{j}\boldsymbol{T}\right) \tag{49}$$

Let $\boldsymbol{U}_i = {}^{i-1}_{i}\boldsymbol{T}\,{}^{i}_{i+1}\boldsymbol{T} \cdots {}^{n}_{n+1}\boldsymbol{T}$, $(i = 1, 2, \cdots n+1)$, $\boldsymbol{U}_{n+2} = \boldsymbol{I}_4$(i.e. a 4×4 unit matrix), we can know that $\boldsymbol{U}_i$ is homogeneous transformation matrix, and it's general formula can be represented as $\boldsymbol{U}_i = \begin{bmatrix} \boldsymbol{n}_i^u & \boldsymbol{o}_i^u & \boldsymbol{a}_i^u & \boldsymbol{p}_i^u \\ 0 & 0 & 0 & 1 \end{bmatrix}$. We bring $\boldsymbol{U}_i$ into (49), and (49) can be simplified as

$$\boldsymbol{\Delta} = \sum_{i=0}^{n} (\boldsymbol{U}_{i+1})^{-1} \cdot \boldsymbol{\Delta}_i \cdot \boldsymbol{U}_{i+1} \tag{50}$$

Then the position/attitude error model of the manipulator can be derived from (50)

$$\boldsymbol{D} = \begin{bmatrix} d_x \\ d_y \\ d_z \\ \delta_x \\ \delta_y \\ \delta_z \end{bmatrix} = \sum_{i=1}^{n+1} \begin{bmatrix} (\boldsymbol{n}_{i+1}^u)^{\mathrm{T}} & (\boldsymbol{p}_{i+1}^u \times \boldsymbol{n}_{i+1}^u)^{\mathrm{T}} \\ (\boldsymbol{o}_{i+1}^u)^{\mathrm{T}} & (\boldsymbol{p}_{i+1}^u \times \boldsymbol{o}_{i+1}^u)^{\mathrm{T}} \\ (\boldsymbol{a}_{i+1}^u)^{\mathrm{T}} & (\boldsymbol{p}_{i+1}^u \times \boldsymbol{a}_{i+1}^u)^{\mathrm{T}} \\ \boldsymbol{0}_{1\times3} & (\boldsymbol{n}_{i+1}^u)^{\mathrm{T}} \\ \boldsymbol{0}_{1\times3} & (\boldsymbol{o}_{i+1}^u)^{\mathrm{T}} \\ \boldsymbol{0}_{1\times3} & (\boldsymbol{a}_{i+1}^u)^{\mathrm{T}} \end{bmatrix} \begin{bmatrix} d_{ix} \\ d_{iy} \\ d_{iz} \\ \delta_{ix} \\ \delta_{iy} \\ \delta_{iz} \end{bmatrix} \tag{51}$$

Bring (44) into (51), then the complete form of position/attitude error model is (52), as shown at the top of this page, where $\boldsymbol{J}_i \in \Re^{6\times5}$ is error Jacobian matrix, $\boldsymbol{e}_i \in \Re^{5\times1}$ is vector of kinematic parameter errors.

REFERENCES

[1] G. Chen, T. Li, M. Chu, Q. X. Jia, and H. X. Sun, "Review on kinematics calibration technology of serial robots," *Int. J. Precis. Eng. Manuf.*, vol. 15, no. 8, pp. 1759–1774, Aug. 2014.
[2] T. Sun, B. Lian, J. Zhang, and Y. Song, "Kinematic calibration of a 2-DoF over-constrained parallel mechanism using real inverse kinematics," *IEEE Access*, vol. 6, pp. 67752–67761, 2018.
[3] G. B. Gao, G. Q. Sun, J. Na, Y. Guo, and X. Wu, "Structural parameter identification for 6 DOF industrial robots," *Mech. Syst. Signal Process.*, vol. 113, pp. 145–155, Dec. 2018.
[4] Z. H. Jiang, W. G. Zhou, H. Li, Y. Mo, W. C. Ni, and Q. Huang, "A new kind of accurate calibration method for robotic kinematic parameters based on the extended Kalman and particle filter algorithm," *IEEE Trans. Ind. Electron.*, vol. 65, no. 4, pp. 3337–3345, Apr. 2018.
[5] Y. Zeng, W. Tian, and W. Liao, "Positional error similarity analysis for error compensation of industrial robots," *Robot. Comput.-Integr. Manuf.*, vol. 42, pp. 113–120, Dec. 2016.
[6] A. Joubair and I. A. Bonev, "Kinematic calibration of a six-axis serial robot using distance and sphere constraints," *Int. J. Adv. Manuf. Technol.*, vol. 77, nos. 1–4, pp. 515–523, Mar. 2015.
[7] A. Joubair and I. A. Bonev, "Comparison of the efficiency of five observability indices for robot calibration," *Mechanism Mach. Theory*, vol. 70, pp. 254–265, Dec. 2013.
[8] M. Hafezipour and S. Khodayga, "An uncertainty analysis method for error reduction in end-effector of spatial robots with joint clearances and link dimension deviations," *Int. J. Comput. Integr. Manuf.*, vol. 30, no. 6, pp. 653–663, 2017.
[9] C. L. Collins and M. L. Robinson, "Accuracy analysis and validation of the Mars science laboratory (MSL) robotic arm," in *Proc. ASME Int. Design Eng. Tech. Conf./Comput. Inf. Eng. Conf. (IDEC/CIE)*, Portland, OR, USA, 2014, pp. 1–10.
[10] T. Gayral and D. Daney, "A sufficient condition for parameter identifiability in robotic calibration," in *Proc. 6th Int. Workshop Comput. Kinematic (CK)*, Barcelona, Spain, 2014, pp. 131–138.
[11] W. Wang, H. Song, Z. Yan, L. Sun, and Z. Du, "A universal index and an improved PSO algorithm for optimal pose selection in kinematic calibration of a novel surgical robot," *Robot. Comput.-Integr. Manuf.*, vol. 50, pp. 90–101, Apr. 2018.

[12] J. H. Borm and C.-H. Menq, "Determination of optimal measurement configurations for robot calibration based on observability measure," *Int. J. Robot. Res.*, vol. 10, no. 1, pp. 51–63, Feb. 1991.

[13] C.-H. Menq, J.-H. Borm, and J. Z. Lai, "Identification and observability measure of a basis set of error parameters in robot calibration," *J. Mech., Transmiss., Autom. Des.*, vol. 111, no. 4, pp. 513–518, Dec. 1989.

[14] M. R. Driels and U. S. Pathre, "Significance of observation strategy on the design of robot calibration experiments," *J. Robot. Syst.*, vol. 7, no. 2, pp. 197–223, Apr. 1990.

[15] A. Nahvi, J. M. Hollerbach, and V. Hayward, "Calibration of a parallel robot using multiple kinematic closed loops," in *Proc. IEEE Int. Conf. Robot. Autom. (ICRA)*, May 1994, pp. 407–412.

[16] A. Nahvi and J. M. Hollerbach, "The noise amplification index for optimal pose selection in robot calibration," in *Proc. IEEE Int. Conf. Robot. Autom. (ICRA)*, Apr. 1996, pp. 647–654.

[17] Y. Sun and J. M. Hollerbach, "Observability index selection for robot calibration," in *Proc. IEEE Int. Conf. Robot. Autom. (ICRA)*, Pasadena, CA, USA, May 2008, pp. 831–836.

[18] A. Joubair, L. F. Zhao, P. Bigras, and I. A. Bonev, "Use of a force-torque sensor for self-calibration of a 6-DOF medical robot," *Sensors*, vol. 16, no. 6, p. 798, Jun. 2016.

[19] T. Li, K. Sun, Z.-W. Xie, and H. Liu, "Optimal measurement configurations for kinematic calibration of six-DOF serial robot," *J. Central South Univ. Technol.*, vol. 18, no. 3, pp. 618–626, Jun. 2011.

[20] Q. Jia, S. Wang, G. Chen, L. Wang, and H. Sun, "A novel optimal design of measurement configurations in robot calibration," *Math. Problems Eng.*, vol. 2018, May 2018, Art. no. 4689710.

[21] D. S. Wang, J. Wang, X. L. Zhu, and Y. Shao, "Determination of optimal measurement configurations for polishing robot calibration," *Int. J. Model., Identificat. Control*, vol. 21, no. 2, pp. 211–222, 2014.

[22] S. Aoyagi, A. Kohama, Y. Nakata, Y. Hayano, and M. Suzuki, "Improvement of robot accuracy by calibrating kinematic model using a laser tracking system-compensation of non-geometric errors using neural networks and selection of optimal measuring points using genetic algorithm," in *Proc. IEEE/RSJ Int. Conf. Intell. Robots Syst. (IROS)*, Oct. 2010, pp. 5660–5665.

[23] Y. Wu, A. Klimchik, S. Caro, B. Furet, and A. Pashkevich, "Geometric calibration of industrial robots using enhanced partial pose measurements and design of experiments," *Robot. Comput.-Integr. Manuf.*, vol. 35, pp. 151–168, Oct. 2015.

[24] T. J. Mitchell, "Computer construction of 'D-optimal' first-order designs," *Technometrics*, vol. 16, no. 2, pp. 211–220, May 1974.

[25] H. Wang, T. Gao, J. Kinugawa, and K. Kosuge, "Finding measurement configurations for accurate robot calibration: Validation with a cable-driven robot," *IEEE Trans. Robot.*, vol. 33, no. 5, pp. 1156–1169, Oct. 2017.

[26] S. Patel and T. Sobh, "Manipulator performance measures—A comprehensive literature survey," *J. Intell. Robot. Syst.*, vol. 77, nos. 3–4, pp. 547–570, Mar. 2015.

[27] Y. Liu, Z. Zhang, and E. Ma, "Some methods of measuring the uniform character of finite point sets," *J. Capital Normal Univ. (Natural Sci. Ed.)*, vol. 18, no. 3, pp. 12–16, 1997.

[28] W. K. Veitschegger and C. H. Wu, "Robot accuracy analysis based on kinematics," *IEEE J. Robot. Autom.*, vol. RA-2, no. 3, pp. 171–179, Sep. 1986.

GANG CHEN (M'17) received the B.S. degree in mechanical design-manufacture and automation from the Beijing Institute of Petrochemical Technology, Beijing, China, in 2004, and the Ph.D. degree in mechatronic engineering from the Beijing University of Posts and Telecommunications, Beijing, in 2011.

He is currently an Associate Professor with the School of Automation, Beijing University of Posts and Telecommunications. His research interests include space robotics, motion planning, and control method.

LEI WANG received the B.S. degree in mechanical engineering and automation from the Beijing University of Posts and Telecommunications, Beijing, China, in 2016, where she is currently pursuing the master's degree in mechatronic engineering.

Her research interests include space robotics, kinematic calibration, and accuracy compensation method.

BONAN YUAN received the B.S. degree in mechanical engineering and automation from the Beijing University of Posts and Telecommunications, Beijing, China, in 2015, where he is currently pursuing the Ph.D. degree in mechatronic engineering.

His research interests include space robotics, failure detection and recovery, and robot control method.

DAN LIU was born in Hunan, China. She received the B.S. degree in mechanical engineering from the Beijing University of Posts and Telecommunications, Beijing, China, in 2017, where she is currently pursuing the M.S. degree in mechanical engineering.

Her research interests include space robotics, collision detection, and path planning method.